Soil Biology and Biochemistry 216 (2026) 110110

Contents lists available at ScienceDirect

Soil Biology and Biochemistry

journal homepage: www.elsevier.com/locate/soilbio

Root exudate-induced priming of CO_2 and CH_4 in a thawing permafrost peatland

Marie Mollenkopf [a,b,c], Sylvain Monteux [d,e], Ellen Dorrepaal [f], Birgit Wild [e,g], Joachim Kilian [h], Mark Stahl [h], Andreas Kappler [a,i], E. Marie Muehe [b,c,*]

[a] Geomicrobiology, Department of Geosciences, University of Tübingen, Tübingen, Germany
[b] Plant Biogeochemistry, Helmholtz Centre for Environmental Research -UFZ, Leipzig, Germany
[c] Plant Biogeochemistry, Department of Geosciences, University of Tübingen, Tübingen, Germany
[d] Tromsø Museum, UiT the Arctic University of Norway, Tromsø, Norway
[e] Bolin Centre for Climate Research, Stockholm University, Stockholm, Sweden
[f] Departement of Ecology and Environmental Science, Climate Impacts Research Centre, University of Umeå, Abisko, Sweden
[g] Department of Environmental Science, Stockholm University, Stockholm, Sweden
[h] Analytics Unit, Centre for Plant Molecular Biology, University of Tübingen, Tübingen, Germany
[i] Cluster of Excellence: EXC 2124: Controlling Microbes to Fight Infection, Tübingen, Germany

ARTICLE INFO

Keywords:
Biogeochemical cycles
Greenhouse gases
Root exudation
Microbes
Methanogens
Iron-carbon mobilization

ABSTRACT

Arctic permafrost faces multiple interactive changes in thaw, drainage, and vegetation shift due to climate warming. Thaw-induced waterlogging can shift vegetation from shrubs to graminoids, altering greenhouse gas emissions. This study aims to quantify and mechanistically explain how vegetation-specific root exudates amplify or dampen greenhouse gas emissions from Arctic permafrost during thaw and drainage transitions. Using field observations and soil incubations, we show that environmentally relevant concentrations of root organic exudates (15% of dissolved organic carbon), obtained from thaw stage-specific plants, altered greenhouse gas fluxes under site-realistic redox conditions. Graminoid exudates were richer in sugars and carboxylates, whereas shrub exudates were richer in amino acids. In thawed, anoxic permafrost soil incubations, graminoid exudates stimulated the emission of 51% more CO_2 and 83% more CH_4 compared to the absence of exudates. In intact, drained permafrost soil, shrub exudates stimulated 14% more CO_2 and negligible CH_4 compared to untreated soils. Geochemical and microbial analyses revealed that soil, including their hydrology, and exudate differences drove exudate and soil organic matter decomposition. These soil incubation findings were supported by field measurements: Bare locations per soil-habitat provided baseline greenhouse gas fluxes in relation to each soil's properties of moisture and geochemistry. Vegetation by graminoids increased greenhouse gas emissions from thawed permafrost soils significantly while shrubs barely affected greenhouse gas emissions from drained permafrost soils. Collectively, this study shows that thaw-specific vegetation shapes greenhouse gas fluxes, indicating that vegetation shifts can intensify radiative forcing beyond the known direct effect of permafrost thaw and associated hydrological transitions. Clarifying the context-dependence and mechanisms underlying these distinct exudate effects may improve projections of Arctic terrestrial climate feedback.

1. Introduction

Terrestrial permafrost soils store 1330-1580 Pg of carbon (C) (Schuur et al., 2015; Mishra et al., 2021), a C pool up to 68% greater than the atmosphere (Friedlingstein, 2020). Due to ongoing climate change, permafrost thaw makes previously protected C accessible to microbial degradation (Åkerman and Johansson, 2008; Patzner et al., 2020; Fewster et al., 2022; Smith et al., 2022), thereby releasing greenhouse gases (GHG) (Schädel et al., 2016; Chang et al., 2021). Thawing can drastically alter soil geohydrology, either enhancing drainage or increasing waterlogging (Avis et al., 2011; Quinton et al., 2011). In ice-underlain lowlands, thaw can transform previously elevated, oxic soils into waterlogged and anoxic soils. These inundated conditions favor anaerobic processes like methanogenesis, shifting ecosystem

* Corresponding author. Plant Biogeochemistry, Helmholtz Centre for Environmental Research -UFZ, Permoserstraße 15, 04318, Leipzig, Germany.
E-mail address: eva-marie.muehe@uni-tuebingen.de (E. Marie Muehe).

https://doi.org/10.1016/j.soilbio.2026.110110
Received 21 August 2025; Received in revised form 31 January 2026; Accepted 4 February 2026
Available online 5 February 2026

emissions from predominantly CO_2 toward CH_4. For example, at Stordalen Mire (northern Sweden), growing-season chamber data revealed CH_4 emissions increasing from ~2 mg C m^{-2} d^{-1} in raised palsa to ~119 mg C m^{-2} d^{-1} in inundated thawed fen, while net CO_2 uptake shifted from 184 to 652 mg C m^{-2} d^{-1}, indicating a substantially larger CH_4 contribution to the C gas budget with thaw and waterlogging (Bäckstrand et al., 2010). Concurrent with these soil transitions, thaw alters plant community composition, further affecting soil biogeochemistry and GHG release (Jorgenson et al., 2001; Christensen et al., 2004; Malmer et al., 2005; Heijmans et al., 2022; Varner et al., 2022).

In drained permafrost soils, perennial dwarf shrub such as *Betula nana* (L.) and *Andromeda polifolia* (L.), can dominate, characterized by branched roots typically limited to the upper 30 cm (Malmer et al., 2005; Iversen et al., 2015; Blume-Werry et al., 2019). They develop coarse, woody roots that live for decades and are used for transport (xylem/phloem movement of water, nutrients, and organic carbon (OC)) and storage (e.g. carbohydrate reserves), alongside resource-acquisitive fine roots with a life span of around 5 years (Iversen et al., 2015; Blume-Werry et al., 2019). Following thaw-induced inundation, shrubs are replaced by hypoxia-tolerate graminoids such as *Carex spp.* and *Eriophorum spp*. (Zoltai, 1993; Beilman, 2001; Malmer et al., 2005; Johansson et al., 2006). These graminoids develop elongated, air-conducting (aerenchyma) roots that penetrate the saturated, anoxic zone below the water table up to 60 cm into the peat, and they exude large amounts of organic acids during their shorter (1-2 year) lifespan (Saarnio et al., 2004; Ström et al., 2012; Iversen et al., 2015; Blume--Werry et al., 2019). Upon their decay in winter, graminoids contribute organic material to the top soil and the rhizosphere (Iversen et al., 2015). Differences in root architecture and exudation patterns between shrubs and graminoids likely influence soil biogeochemistry (Varner et al., 2022; Määttä and Malhotra, 2024).

Plants can substantially accelerate soil organic carbon (SOC) losses through the rhizosphere priming effect (RPE), the stimulation of SOC mineralization by microbial and chemical processes near roots (Kuzyakov, 2010; Xu and Zhou, 2011; Keiluweit et al., 2015; Natali et al., 2019; Malhotra et al., 2020). Roots release a complex mixture of exudates including protons, soluble inorganic compounds like CO_2, and O_2, and OC substrates like sugars, carboxylates, organic acids, amino acids, proteins, lipids, and flavonoids (Jones et al., 2009). The amount and composition of these root exudates depend on plant species, developmental stage, and environmental conditions (Iversen et al., 2015; Proctor and He, 2017; Blume-Werry et al., 2019; Waldo et al., 2019; Wegner et al., 2025; Jilling et al., 2021). In northern permafrost systems, RPE may increase microbial respiration of SOC by 12% based on a model estimate (Keuper et al., 2020). Recent experimental evidence demonstrates positive RPE in permafrost soils (Street et al., 2020; He et al., 2023; Friggens et al., 2025), with root activity increasing SOC losses by ~30% and effects persisting longer in permafrost than in active-layer soils (Friggens et al., 2025). Other studies report resistance of (sub-)arctic soils to RPE (Verbrigghe et al., 2022; Wild et al., 2023). Key uncertainties remain regarding how natural variation in plant species and realistic root exudate chemistry, modulate GHG emissions and RPE under field-relevant conditions across thaw gradients.

Besides enhancing CO_2 emissions, root exudates affect anaerobic microbial processes, potentially altering CH_4 and N_2O emissions. Labile exudates like glucose or acetate can lower thermodynamic constraints under anoxic conditions (LaRowe and Van Cappellen, 2011; Sutton--Grier et al., 2011; Keiluweit et al., 2016), facilitating fermentation, Fe (III) reduction and methanogenesis, thereby increasing CH_4 emissions, also found in organic-rich permafrost soils (Joabsson et al., 1999; Jean Le Mer, 2001; Waldo et al., 2019). Other compounds like citrate or oxalate can chemically dissolve minerals, mobilizing metals (e.g., Fe(III)) through complexation, thereby enhancing RPE by releasing associated OC (Keiluweit et al., 2015; Jilling et al., 2021; Li et al., 2021) or potentially suppressing methanogenesis by providing alternative electron acceptors (Sutton-Grier and Megonigal, 2011; Määttä and Malhotra, 2024).

Because Arctic permafrost soils store up to ~50% of global SOC (Tarnocai et al., 2009), RPE may have disproportionate consequences for CO_2 and CH_4 emissions at the global scale (Wild et al., 2023). Yet, experimental evidence on (natural) root exudation and its impacts on soil microbial activity and GHG production remains limited (Wild et al., 2023; Wegner et al., 2025) and knowledge on CH_4 priming in particular is still scarce and largely confined to agricultural systems such as paddy soils (Kim et al., 2016; Wei et al., 2021). This gap is especially critical in Arctic permafrost landscapes, where thaw simultaneously alters hydrology (wet vs. drained conditions) and vegetation, likely shifting both the amount and quality of plant-derived inputs along thaw gradients. Moreover, many studies use simple sugars or organic acids as proxies for exudates, which poorly capture the chemical diversity and the spatial and temporal dynamics of natural root exudation, potentially biasing priming estimates (Friggens et al., 2025; Wegner et al., 2025). More realistic mechanistic studies are needed to accurately predict future Arctic CO_2 and CH_4 emissions, particularly considering the rapid and interacting changes in permafrost thaw, drainage, and vegetation.

Addressing these knowledge gaps, we posed two linked hypotheses. First, thaw-induced shifts in plant community composition will influence GHG emissions in situ on top of known soil hydrology impacts. Second, water-logged, thawed fen with graminoids will exhibit higher CH_4 fluxes than adjacent bare thawed surfaces, whereas drained, oxic palsa will cause negligible CH_4 fluxes and only modest vegetation effects on CO_2. These hypotheses were tested with dark-chamber fluxes across bare versus vegetated plots in the thawed and drained habitats at Stordalen Mire, Sweden. For mechanistic understanding of these flux data from the field, two targeted research questions were examined 1) how root exudate composition varied along a permafrost thaw gradient and 2) how these exudates affected soil biogeochemistry and GHG release differently in drained versus thawed permafrost soils. To do so, active-layer soils from intact palsa (drained permafrost soil) and collapsed palsa (thawed permafrost soil) were incubated under their site-relevant conditions: oxic for drained and anoxic for thawed permafrost soil. Soils were amended with root exudates from dominant plant species, *Andromeda polifolia (A. polifolia)* shrubs (hereafter termed *A. polifolia* exudates) for the drained permafrost soil, and graminoids (hereafter termed graminoid exudates) for the thawed soils. To isolate compositional effects, incubations included soil-derived OC from site-specific soil extractions (hereafter termed drained permafrost soil dissolved organic carbon (DOC) and thawed permafrost soil DOC), alongside non-amended controls (hereafter termed control). Because root exudation is continuous in situ, our incubation mainly targets immediate microbial and biogeochemical responses to distinct exudate inputs. This framework clarifies mechanistic controls on CO_2 and CH_4, linking soil moisture, plant species, and plant-specific exudate chemistry to the resulting soil-microbe processes.

2. Materials and methods

2.1. Study site and field work

Soils and plant root exudates were sampled in a well-studied, permafrost palsa peatland in Stordalen mire near Abisko, Sweden (68° 20′N, 19° 03′E) (Fig. S1) in September 2022. Drained (palsa) and thawed (fen) locations were ~30 m apart. Intact permafrost palsas are dominated by mosses and lichen as well as dwarf shrubs (e.g. *Empetrum spp., Rubus chamaemorus, Andromeda polifolia)*. Thaw-induced changes in hydrology formed sub-habitats: an ombrotrophic *Sphagnum* bog underlain by silty permafrost that upon thaw slopes down to a fully inundated thawed permafrost soil covered by grasses and sedges (e.g. *Eriophorum vaginatum, Eriophorum angustifolium, Carex ssp.)*. The air temperature was around 10 °C during the field sampling time and matched the average of September temperatures of the last six years whereas precipitation in the sampling year was high compared to the average of the

last six years. Meteorological data was provided by the Integrated Carbon Observatory Station (ICOS) portal (ICOS Sweden et al., 2021a–d, 2022, 2023); the full dataset citations and persistent identifiers are provided in the References).

The overall approach of this study is illustrated in Fig. 1. Field measurements of GHG emissions (CO_2, CH_4, N_2O) were conducted using dark static chambers (~40x40 × 40 cm), covered with opaque HDPE designed to exclude light and suppress photosynthesis. Thus, dark-chamber fluxes quantify ecosystem respiration (soil + root) and any anaerobic production (e.g., CH_4) within the footprint. Chambers were placed onto square collars (~40 × 40 cm footprint, inserted ~20 cm into the soil) installed 24 h before measurements to minimize disturbances of the soil and atmosphere. Each collar had rims filled with water to create a gas-tight seal. Collars were inserted by hand to avoid severing major shrub stems; the 20 cm insertion depth and water seal minimized lateral diffusion artefacts. Sampling points represented bare and vegetated conditions at drained and thawed sites. For each vegetation state and habitat, three different locations were selected and two independent closure series on separate days were performed. Vegetation density was quantitatively classified based on plant cover determined through image analysis using ImageJ software: bare conditions had less than 10% vegetation cover, while vegetated conditions had cover above 80%. Gas samples were periodically taken from chamber headspaces every 5-15 min, stored in evacuated exetainers, and analyzed using gas chromatography (for analytical details, see "Gas analyses and calculations").

2.2. Soil sampling, soil characterization, and organic carbon extraction

For the drained and thawed permafrost sites, we sampled soil directly above the permafrost (~40 cm), thus, at the bottom of the active layer. The soil was transported from the field site to the Abisko research station within 2 h. Soils were stored at 4 °C in the dark for ~3 months until used for soil characterization, OC extractions, and the experiment.

For soil characterization, soil pH was determined in triplicates by suspending wet soil in a 1:2.5 soil:water ratio with an InLab Easy pH probe (Mettler Toledo, USA) after 1 h. Water content was calculated from the wet soil weight compared to the oven-dried (105 °C) soil weight. Due to possible interferences during texture analysis, OC was purged from the soil by treatment with H_2O_2 according to Gee and Or (2002). Subsequently, soil texture was classified for three replicates by wet sieving and sedimentation analysis with a PARIO particle analyser (METERGroup, Germany). Cation exchange capacity (CEC) was determined in triplicates as the sum of the exchangeable base cations (Ca^{2+}, Mg^{2+}, K^+, Na^+, Al^{3+}) extracted with 0.1 M $BaCl_2$ for 4 h at a 1:25 (w/v) ratio (horizontal shaker, 150 rpm, 0.45 µm filtered (PES filter), acidified in 1 M HNO_3) using Microwave Plasma Atomic Emission Spectroscopy (4200 MP-AES, Agilent Technologies, USA). Total (organic) C and N from oven-dried (60 °C) and ground samples were determined by combustion on a soli TOC cube (Elementar, Germany). POC and MAOC were separated using size fractionation based on chemical dispersion (Cambardella and Elliott, 1992; Cotrufo et al., 2019). In brief, 10 g of air-dried, 2-mm-sieved soil was shaken in 50 mL of 0.5% sodium hexametaphosphate solution for 18 h and subsequently rinsed onto a 53 µm sieve. The organic material passing through was defined as MAOM, and the remaining fraction was defined as POM. OC of the fractions was analyzed on a soli TOC (Elementar, Germany).

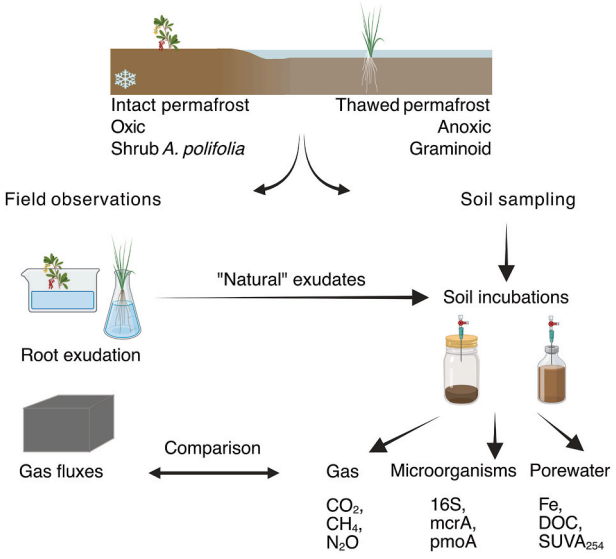

Fig. 1. Flowchart illustrating the approach of this study.

Soil OC extractions for use in the incubation experiment were performed on the bulk soil and on the soil attached/close to the roots (rhizosphere). Bulk soil was used to mimic the native C. The rhizosphere soil extract resembles an intermediate between root exudates and bulk soil extract and is portrayed in the supplements for reference. Of each soil type, 75 g was weighed into sterile Schott bottles (300 °C, 8 h), degassed with N_2 and extracted in 750 ml of anoxic artificial rainwater (Table S1) for 24 h on an overhead shaker with 10 spins per min. The extraction solution was centrifuged (15 min at 4000 rpm), and the supernatant was sterile-filtered (0.22 µm, Merck Millipore, PES Steritop).

2.3. Plant exudate sampling

The plant species chosen for this study, *Andromeda polifolia* (shrubs) for drained permafrost soils and *Eriophorum angustifolium* and *Carex* spp. (graminoids) for thawed permafrost soils, represent dominant vegetation types in their respective habitats, making them suitable representative plants to examine vegetation-driven biogeochemical shifts in Arctic permafrost ecosystems. Thus, the representative plants *Andromeda polifolia* from drained permafrost soil and *Eriophorum angustifolium, Carex ssp.* from the thawed permafrost soil were excavated from the field and arrived at the Abisko research station within 2 h. Plant roots were gently cleaned from the remaining soil by rinsing with tap water and pre-incubated in tap water for 18 h under a plant lamp to assure plant health. The plant roots were dried with a paper tissue and placed into a hydroponic solution with artificial rainwater (Table S1) for 3 h beneath a plant lamp to collect root-exuded OC (Oburger and Jones, 2018), temperature under the plant lamb was stable throughout the incubation for exudate sampling. Sampling in September coincides with late-season physiology; graminoids were senescing while *A. polifolia* remained evergreen, which likely reduced graminoid exudation amounts and shifted composition; we therefore treat exudates as conservative late-season representations.

After exudate collection, plants were removed from the hydroponic solution, and the roots were dried with a paper tissue. Roots were separated from shoots, and each fraction weighed for wet biomass. Tissues were dried at 60 °C for 3 days and weighed for dry biomass, which can be used to normalize metabolite data to plant habitus. The hydroponic solution containing exudates was sterile-filtered (0.22 µm, Merck Millipore, PES Steritop) and frozen at −20 °C until analyses. Prior to the experiment exudates were pooled within functional group (~20 single plants per group; shrubs: *A. polifolia*; graminoids: *E. angustifolium* + *Carex* spp.) and concentrated by vacuum centrifugation at room temperature. The exudates analyzed in this study reflect species-specific metabolic profiles generated under standardized light conditions, allowing a direct comparison of inherent differences among plant species rather than responses to variable environmental factors in the field.

2.4. Organic carbon characterization

Root exudates as well as extracts of bulk and rhizosphere soil were concentrated by vacuum centrifugation to reach a DOC concentration of approximately 150 mg L^{-1}. Mixed exudate pools were then distributed

on a C-equivalent basis to increase DOC by 15% relative to the control in each incubation (identical DOC increase across treatments and soils).

The aromaticity of root exudates, bulk, and rhizosphere soil extracts were characterized in biological triplicates photospectrometrically by using the specific UV absorbance (SUVA) at $\lambda = 254$ nm (Specord 50 plus, Analytik Jena, Germany) after running three blanks of ultra-pure water. Known root-exuded and soil metabolites (AminiTabrizi et al., 2020; Williams et al., 2022) (Table S2) were determined using gas chromatography-mass spectrometry (GC-MS) (Shimadzu GC/MS TQ 8040). Metabolites were analyzed either by headspace injection or as liquid samples after derivatization and addition of octanol or ^{13}C-glucose as internal standard, respectively (details in Text S1). Metabolite concentrations were quantified with an 8-point external calibration containing standards of all targeted analytes, ranging from 20 to 10^7 pmol. (Details on procedure in Text S1). R (4.2.2) (Team, 2024) was used to calculate relative peak areas and the concentrations of metabolites. Given sample treatment, derivatization and bias in metabolite detection, GC-MS-based metabolite data should only be regarded as semi-quantitative, thus heatmaps and no absolute graphs are presented.

The nominal oxidation state of metabolite OC ($NOSC_M$) was calculated from the GCxMS-derived metabolites using the following formula proposed by LaRowe and Van Cappellen (2011) and Riedel et al. (2012):

$$NOSC = 4 - \left[\frac{4c + h - 3n - 2o - 2s}{c}\right]$$

where c, h, n, o, and s refer to the stochiometric number of C, hydrogen, oxygen, and sulfur atoms per formula, respectively.

2.5. Soil incubation studies and sampling

A lab incubation experiment was set up under oxic conditions for the drained permafrost soil and under anoxic conditions for the thawed permafrost soil. Each was amended with bulk soil extract, the corresponding root exudate (*A. polifolia* for drained permafrost soil, graminoid for thawed permafrost soil), or left unamended as a control, in three replicates (Fig. S2), with three biological replicates per treatment and soil. The chosen OC amendment level, increasing soil DOC by 15%, was derived from measured exudation rates during hydroponic experiments combined with estimates of root biomass densities Monteux et al. (2018) in the respective field habitats. It was also consistent among all treatments, allowing their comparison. Differences in the timing of the sampling and the duration of the experiment between the two experiments were necessary due to the much faster response of the oxic than the anoxic soil incubation.

The oxic microcosm study using drained permafrost soil was performed in 500 mL pre-sterilized (300 °C for 8 h) mason jars (Ball, USA), which were closed with breathe-easy foils (Diversified Biotech, USA) that allow gas exchange (Fig. S2). The jars were filled with 100 g of 2 mm wet-sieved drained permafrost soil and pre-incubated for 2 weeks to minimize artefacts from soil preparation. At the start of the experiment, *A. polifolia* exudates, *A. polifolia* rhizosphere or bulk soil extracts were sprayed onto the soil, followed by thorough mixing. Thereby, exudates were gently mixed into the soil to ensure homogenous distribution. As a control without C input, artificial rainwater was added to assure similar ionic strength as the exudate mixes (composition provided in Table S1). For GHG emission quantification, breathe-easy foils were removed, and jar lids with mounted gas sampling ports were attached. Three headspace gas samples of 4 mL each were taken with gas-tight syringes at 0, 20, and 40 min within a 40-min incubation period after lid closing. Gas samples were injected into helium-flushed (He 5.0, Westfalen Gas, Germany) 12 mL exetainers. Total amounts of gas samples were chosen to not exceed 5% of headspace volume to avoid bias by underpressure in the vial. For liquid phase analyses, 1 g of soil was sampled from six different locations in the top 5 cm of the soil under an N_2 stream, put into 50 mL serum bottles, and brought anoxically to the N_2-glovebox (UNIlab Pro, MBraun, Germany). Soils were extracted for 1 h in 10 mL of anoxic ultrapure water on a rolling shaker (20 rpm). The slurry was centrifuged, and supernatants filtered through 0.22 µm, ultrapure water flushed PES filters. The filtered supernatant was analyzed for pH, DOC, nitrogen (N) species, iron (Fe) species and OC characterization (aromaticity). To extract short-range order Fe minerals, 0.2 g of soil was weighed into 2 mL Eppendorf tubes and extracted with 1.5 mL of 0.5 M HCl for 3 h. Tubes were centrifuged and supernatants were diluted in 1 M HCl in a 1:1 dilution. Soil was additionally sampled for microbial analyses in sterilized 2 mL tubes and immediately frozen at −80 °C. The water content of 36% in the jars was adjusted every two to three days based on weight.

The anoxic microcosm study using thawed permafrost soil was performed in pre-sterilized (300 °C for 8 h) 250 mL serum bottles with 20 g of wet, homogenized soil (Fig. S3). The bottles were butyl-stoppered, and the headspace was exchanged with N_2 three times. 80 mL of anoxic artificial rainwater (Table S1) was added inside the N_2-glovebox, and samples pre-incubated for three weeks to minimize artefacts from soil preparation and to ensure anoxic slurry conditions. After the pre-incubation, anoxic substrates (artificial rainwater as control without C input, graminoid exudates, graminoid rhizosphere, and bulk soil extracts) were added to the bottles to increase the DOC concentrations by 15%. Exudates were injected anoxically into the slurries to ensure homogenous distribution and avoid artefacts by introducing oxygen to the system. To avoid accumulation of CO_2 or CH_4 in the anoxic, N_2-flushed headspace, it was exchanged every 4 h using an automated flush system (Fig. S2). To quantify GHG emissions, four gas samples of 3 mL each were taken from the incubation bottles at regular intervals within a 70-min incubation period and injected into 12 mL exetainers. Soil slurries were sampled anoxically in the N_2-glovebox by taking 3 mL of slurry and centrifuging it for 5 min at 14,000 rpm. The supernatant was aliquoted for pH, DOC, N species, Fe species, and OC characterization (aromaticity). 0.4 mL of soil slurry was weighed into bead tubes (Lysing Matrix E, MP BioMedicals, USA) and immediately frozen at −80 °C until microbial analysis. Measured pH values (Table S3) did not change in a systematic direction during the incubations.

2.6. Gas analyses and calculations

The concentrations of CO_2, CH_4 and N_2O were determined using a gas chromatograph (Thermo Fisher SCIENTIFIC TRACE 1310, Thermo Fisher Waltham, Massachusetts, USA) equipped with two pulsed discharge ionization detectors (PDD). Measured parts per million (ppm) concentrations were corrected for sampling temperature using the ideal gas law. Gas production rates were calculated based on a linear change in headspace gas concentration over time and normalized per g dry soil according to the equations published in Ruser et al. (1998). To facilitate comparison among gases, we additionally report the metric-weighted sum as net CO_2-equivalent flux/emissions (CO_2-eq), also referred to as radiative balance (Neubauer, 2021). CO_2-eq was calculated assuming gas-specific abilities of radiative efficiency and lifetimes in the atmosphere and normalized to the amount of energy absorbed by 1 ton of gas over a given period of time relative to 1 ton of CO_2. CH_4 was assumed to have a warming potential (WP) 30 times higher than CO_2, and N_2O to have a WP 273 times higher than CO_2 (IPCC, 2023). Priming was calculated by resetting the cumulative fluxes to zero once the amount of added C was fully released as GHGs. The subsequent flux increases (or decreases) of the OC treatments were compared relative to the control.

2.7. Aqueous analyses

DOC was quantified in technical triplicates on a multi N/C 2100 (Analytik Jena, Germany). OC aromaticity was determined in technical triplicates using the specific UV absorbance at 254 nm (Specord 50 plus, Analytik Jena, Germany). pH was determined with technical triplicates

using an InLab Easy pH probe (Mettler Toledo, USA). Nitrogen species (nitrite, nitrate, and ammonium) were quantified using flow injection analysis (AA3, Seal analytical, USA). The ferrozine assay (Stookey, 1970) quantified total Fe concentrations and Fe species in technical triplicates spectrophotometrically (MultiskanTM GO, Thermo Fisher Scientific).

2.8. Soil microbial ecology analyses

Time points for sampling for microbial ecology analysis were based on changes in GHG emissions (preincubation, days 1, 3, 17, 27/30 after substrate addition). DNA and RNA were co-extracted from soil slurry pellets (anoxic incubation) as described previously (Lueders et al., 2004). Due to high OC loads in soil samples of the oxic drained permafrost soil incubation, RNA and DNA were extracted respectively with the RNeasy PowerSoil Total RNA Kit and the RNeasy PowerSoil DNA elution Kit (Qiagen, Netherlands)). DNA/RNA contents were quantified with a Qubit 2.0 fluorometer (Thermo Fisher Scientific) and quality checked for 260 nm/280 nm ratios on NanoDrop (Thermo Fisher Scientific). For DNA/RNA co-extracts, RNA was purified from DNA using the Invitrogen™ TURBO DNA-free™ Kit (Thermo Fisher Scientific) and reverse-transcribed into complementary DNA (cDNA) using the Invitrogen™ SuperScript™ III Reverse Transcriptase Kit (Thermo Fisher Scientific). DNA and RNA quality, DNA removal, and cDNA synthesis were checked via PCR using primers 515-F (5′-GTGYCAGCMGCCGCGGTAA-3′) (Parada et al., 2016) and 806-R (5′-GGACTACNVGGGTWTCTAAT-3′) (Apprill et al., 2015) followed by 1% (w/v) ethidium-bromide-died agarose gel.

Gene and transcript copy numbers were quantified with quantitative PCR (qPCR) using 1 × SsoAdvanced Universal SYBR Green Supermix (Bio-Rad Laboratories, Hercules, CA, USA) for 16S rRNA. Functional assays targeted *mcrA* and *pmoA* to track methanogen dynamics, additionally N-cycling markers were not quantified because N_2O fluxes were infrequent and near detection limits (primers in Table S4). Notably, *pmoA* was below quantification in all samples despite positive controls, so we report non-detects. In a 10 μL reaction volume, 1 μL of template DNA and cDNA or a tenfold dilution series of the standard plasmid DNA were annealed gene-specific forward and reverse primers (Table S4). The qPCR programs ran on a CFX Connect Real-Time PCR Detection System (Bio-Rad Laboratories, Hercules, CA, USA). The data analysis was performed using the Bio-Rad CFX Maestro software (Bio-Rad Laboratories, Hercules, CA, USA).

2.9. Data analyses

Means and 1 standard deviations (1SD) were calculated for all analyses except for the microbial functional genes where standard errors were used. For boxplots, black diamonds represent the mean, and the line in the box is the median; whiskers show the Q10 and Q90, and n is the number of datapoints per whisker plot. Statistical analyses were done using IBM SPSS Statistics (Version 27). For incubation data, linear mixed-effects models were fit separately by soil (drained, thawed) and GHG (CO_2, N_2O, CH_4) with treatment (levels: control, bulk-soil DOC, plant exudates), Time (categorical sampling day), and their Treatment × Time interaction as fixed effects, and a random intercept for jar/bottle to account for repeated measures within microcosms. Subsequent, post-hoc tests were performed at a confidence interval of 0.95 to test the significant impact of the different OC substrates on GHG production. Significant differences among C treatments were evaluated using a two-sided *t*-test. Prior to pairwise tests, we assessed normality (Shapiro–Wilk) and variance homogeneity (Levene). When assumptions were violated, we applied Welch's unequal-variance *t*-test instead of transforming the data.

3. Results

3.1. Characteristics of soils

Drained and thawed permafrost soils used in the incubations differed in major soil properties (Table S5). According to the World Reference Base for Soil Resources (WRB), the drained permafrost soil is an acidic gelic Histosol with a pH of 4.1 and 46% SOC. Aromaticity (Specific UV absorbance at 254 nm ($SUVA_{254}$)-based) was 3.8 ± 0.2 L mg^{-1} m^{-1} at ~40 cm depth, 72% of which was particulate organic carbon (POC) (Fig. 2A). The thawed permafrost soil is a Histosol with a pH of 5.4 and 19% SOC content with an aromaticity was 3.0 ± 0.02 L mg^{-1} m^{-1} at ~50 cm depth, of which 55% was mineral-associated organic carbon (MAOC) (Fig. 2A–Table S5, cores in Fig. S1B and C).

3.2. Characteristics or root exudates

Metabolites quantified in drained permafrost soil DOC were enriched in phenolic substances (e.g., benzoic acids) compared to *A. polifolia* exudates with an overall aromaticity of 0.8 ± 0.1 L mg^{-1} m^{-1} that were enriched in amino acids (e.g., alanine, threonine, valine, serine, and glycine), and sugars (specifically fructose and sucrose) compared to both soil extracts (Fig. 2B). Graminoid exudates with an overall aromaticity of 0.4 ± 0.003 L mg^{-1} m^{-1} were enriched in multiple sugars (e.g., xylose, glucose, mannose), in amino acids (specifically arginine and asparagine), and many organic acids, relative to *A. polifolia* exudates. Relative to bulk soil extracts, graminoid exudates were mainly enriched in acetic, propionic, and malic acids. The thawed permafrost soil DOC was enriched in multiple organic acids yet depleted in sugars and amino acids relative to graminoid exudates.

3.3. Exudates stimulate GHG emission during incubation

Field observations demonstrated significant differences in GHG emissions between bare and vegetated soils in thawed permafrost (Fig. 3). Specifically, thawed permafrost vegetated by graminoids emitted 11-times more CO_2 and 400-times more CH_4 compared to bare thawed permafrost (Fig. 3). In contrast, drained permafrost emitted more CO_2 than thawed permafrost and negligible CH_4. However, there were no significant differences between bare and vegetated areas for either CO_2 or CH_4.

Adding OC substrates increased GHG emissions in the thawed but not the drained permafrost soil in the first five days (Fig. 4). Cumulative CO_2 emissions of the drained permafrost soil in the control amounted to 97.2 ± 11.6 μg CO_2 g^{-1} dry soil within five days (Fig. 4A). Addition of drained permafrost soil DOC did not increase cumulative CO_2 emissions from the soil compared to the control. The addition of *A. polifolia* exudates did not significantly increase cumulative CO_2 emissions over the first five days. Cumulative CO_2 emissions of the thawed permafrost soil in the control amounted to 75.5 ± 13.3 μg CO_2 g^{-1} dry soil within five days (Fig. 4B). Addition of thawed permafrost soil DOC tended to increase cumulative CO_2 emissions by 33%. Graminoid exudates significantly increased cumulative CO_2 emissions by 51% relative to the control in the first five days (fixed single effects $p < 0.001$, Table S8, Table S10).

Cumulative net N_2O fluxes of the drained permafrost soil in the control were 25.3 ± 22.1 μg N_2O g^{-1} dry soil within five days (Fig. 4C). None of the OC treatments significantly differed from the control, given the generally large variability of emitted N_2O. Net N_2O production from the thawed permafrost soil under any OC addition was detected only sporadically as single pulses during the incubation; thus, it was impossible to identify trends (Fig. S3D).

As anticipated, given that the drained permafrost soil was oxic, CH_4 fluxes were negligible (Fig. S3E). Cumulative CH_4 emissions of the thawed control were 96.4 ± 94.2 μg CH_4 g^{-1} dry soil within five days (Fig. 4D). The addition of thawed permafrost soil DOC did not result in different CH_4 outputs compared to the control within 5 days. In contrast,

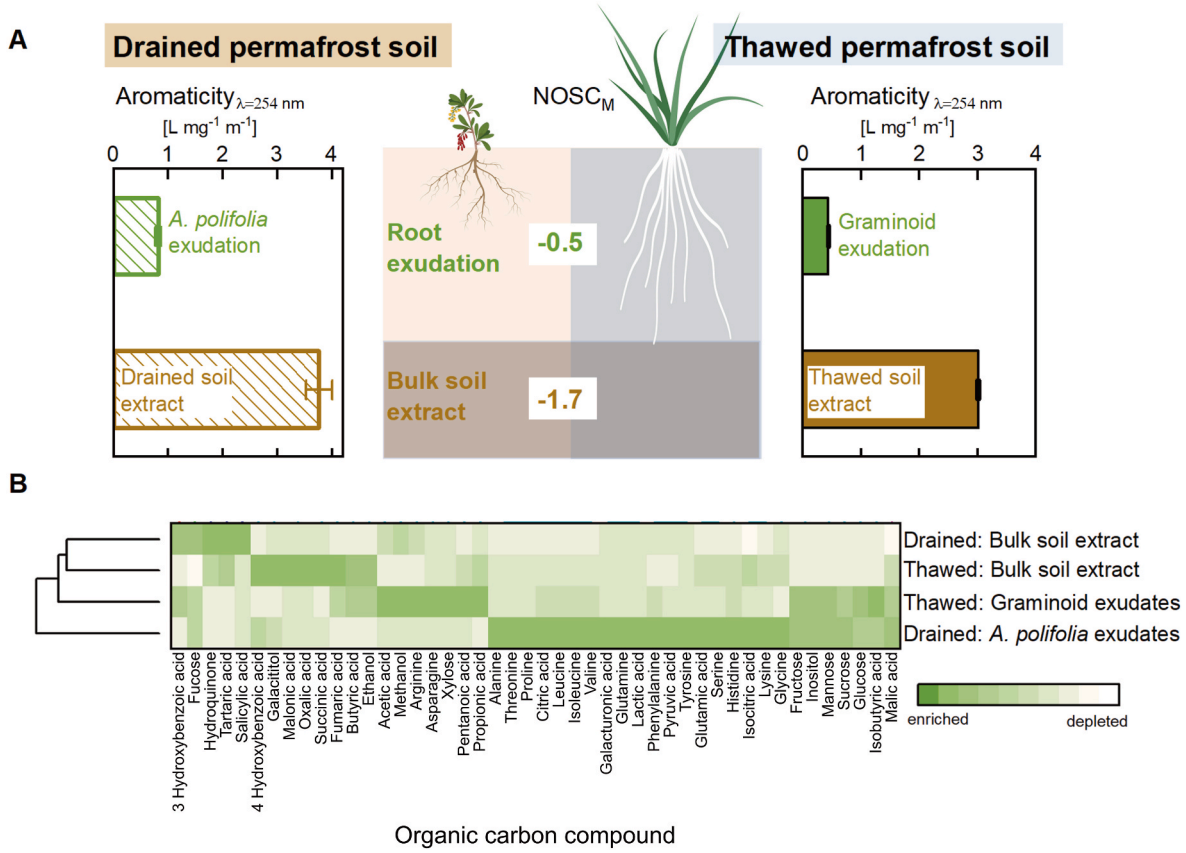

Fig. 2. Characteristics of *A. polifolia* and graminoid exudates, as well as soil extracts from drained and thawed soil obtained from a permafrost thaw profile, Stordalen mire, Abisko, Sweden. (A) Aromaticity and metabolite-specific nominal oxidation state of organic carbon ($NOSC_M$) of root exudates and extracts from drained (left) and thawed (right) soil. (B) Heatmap of metabolites in bulk and plant exudates providing also their relation to one another with a tree (in black lefthand side). Each cell represents the mean of a metabolite obtained from 3 to 4 replicates and normalized to total dissolved organic carbon. Green indicates relative enrichment; white indicates relative depletion. Plants and soils created with BioRender.com. (For interpretation of the references to colour in this figure legend, the reader is referred to the Web version of this article.)

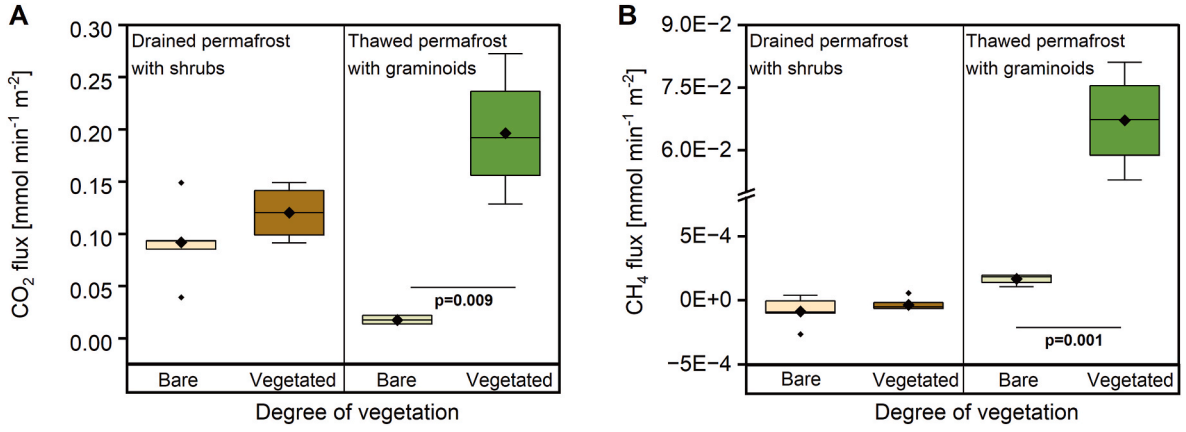

Fig. 3. Field evidence of greenhouse gas emissions in drained and thawed permafrost soils in Stordalen mire near Abisko, Sweden, as affected by shrubs and graminoids. (A) CO_2 and (B) CH_4 fluxes from bare (<10% shrubs and graminoids, respectively) and vegetated locations nearby (>80% shrubs and graminoids, respectively) in drained permafrost soils and thawed permafrost soils. N = 3-6. Significant differences between densely vegetated and bare locations displayed when $p < 0.05$.

adding graminoid OC significantly increased cumulative CH_4 emissions by 83% relative to the control at day five (fixed single effects $p < 0.001$, Table S9).

The net CO_2-eq emission of the GHGs released from the drained and thawed permafrost soil in the control was 122.5 ± 18.1 μg CO_{2eq} g^{-1} dry soil and 171.9 ± 32.6 μg CO_{2eq} g^{-1} dry soil over five days, respectively (Fig. 4E). Neither the addition of soil DOC nor *A. polifolia* exudates to the drained permafrost soil significantly changed the net CO_2-eq emission (−3% for drained permafrost soil DOC, 9% for *A. polifolia* exudates solely due to changes in CO_2 emissions, Fig. 4F). Addition of soil DOC to the thawed permafrost soil tended to increase the net CO_2-eq emission after five days by 23%. Adding graminoid exudates significantly

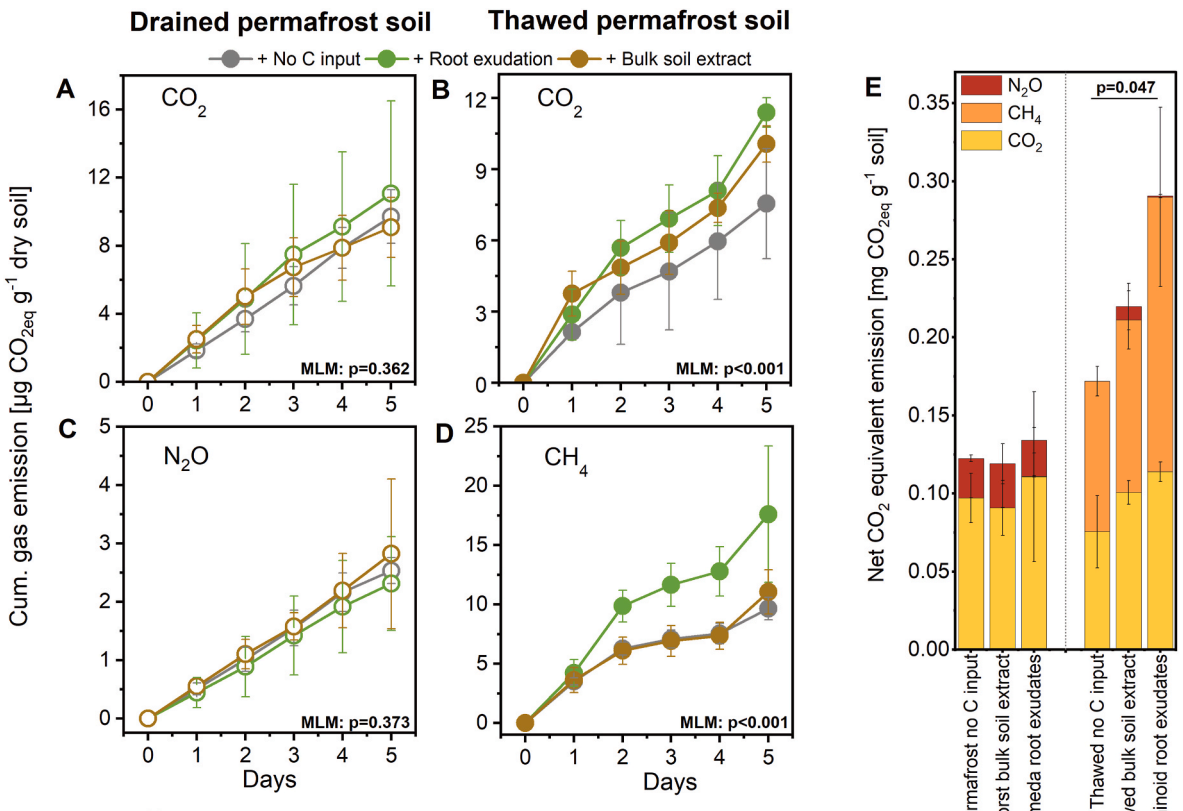

F

Fold change in gas emissions

	Bulk vs Control		Exudates vs Control	
	Drained	Thawed	Drained	Thawed
CO_2	0.93	1.33	1.14	1.51
CH_4	-	1.15	-	1.83
N_2O	1.1	-	0.91	-

Fig. 4. Greenhouse gases emitted from drained and thawed soils, obtained from a permafrost thaw profile in Stordalen mire, Abisko, Sweden exposed to different carbon substrates. (A, B) Cumulative CO_2, (C) N_2O, (D) and CH_4 emitted from drained and thawed soils in the first five days of incubation. For GHG fluxes of the whole incubation period of 48 and 67 days see Fig. S3. Interactions between carbon treatments and GHG emissions are implemented as p-values from mixed linear models (MLM) (Tables S6–S9); Additional t-tests for CO_2 and CH_4 are in Tables S10–11. (E) The net CO_2 equivalent emission of the cumulative GHG formed after 5 days for the control and the additions of bulk soil organic carbon- and root exudates, considering the three major GHGs CO_2, CH_4, and N_2O. Significant differences in OC treatments relative to the control are included when $p < 0.05$ (Table S12). (F) The change in GHG emissions for the soils spiked with bulk SOC and root-exuded OC was calculated relative to control of the cumulative emissions on day 5. Mean ± 1SD, n = 3.

increased the net CO_2-eq emission by 69% relative to the control (Table S12), mainly due to increased CH_4 emissions.

To assess whether priming occurred under environmentally relevant low-C additions, we extended the incubations and calculated relative priming after substrate consumption (Fig. S3, Fig. S8). Here, relative priming is the difference in cumulative flux between the C-amended treatment and the control after the added C pool was fully respired. Values above 0 denote positive priming, while values below 0 imply negative priming (Fig. S8; substrate-consumption timing in Fig. S3). The addition of *A. polifolia* exudates to drained permafrost soil increased the cumulative CO_2 emissions significantly compared to the control over the entire incubation period of 48 days (fixed single effects $p = 0.008$; Table S6) and resulted in positive but insignificant relative priming of 7% (Fig. S8). Adding graminoid exudates to thawed permafrost soils increased CO_2 emissions significantly compared to the control over the entire incubation period of 67 days (fixed single effects $p < 0.001$, Table S8) with a relative positive and significant priming of 13% ($p > 0.001$, Fig. S8). Yet, CH_4 responses separated into two phases: an early increase (days 1–5; Fig. 4D) coincided with higher *mcrA* transcripts at day 1 (Fig. 5C) and an increase in aqueous Fe at days 4–7 (Fig. 6F). Thereafter, CH_4 declined below the control (Fig. S3F), resulting in a net negative priming (Fig. S8). Graminoid exudates decreased CH_4 fluxes significantly (fixed single effects $p < 0.001$, Table S9) relative to the control in the long term; thus, negative relative priming of −40% was observed for CH_4 (Fig. S8). CH_4 priming was not calculated for the drained permafrost soil because CH_4 fluxes were negligible (Fig. S3E). Field CH_4 fluxes can further exceed lab responses obtained from sealed slurry incubations because graminoids' aerenchyma tissues bypass the oxidative layers and diffusion limits transporting CH_4, and water-table fluctuations trigger ebullition (Saarnio et al., 2004; Ramirez et al., 2016).

3.4. Alteration in microbiome dynamics

Analysis focused on community size/activity (16S rRNA genes/transcripts) and methanogen size/activity (*mcrA* genes/transcripts) because the strongest and most consistent gas response occurred for CH_4 under anoxia, whereas N_2O fluxes were sporadic and low, and CO_2 stems from diverse heterotrophs not represented by a single functional marker. OC addition altered prokaryotic abundance and potential activity more in the thawed permafrost soil than in the drained permafrost soil (Fig. 5). Adding either soil DOC and *A. polifolia* exudates to drained permafrost soil did not elicit a significant impact on 16S rRNA gene and transcript copy numbers after day 1 (Fig. 5A). While 16S rRNA gene

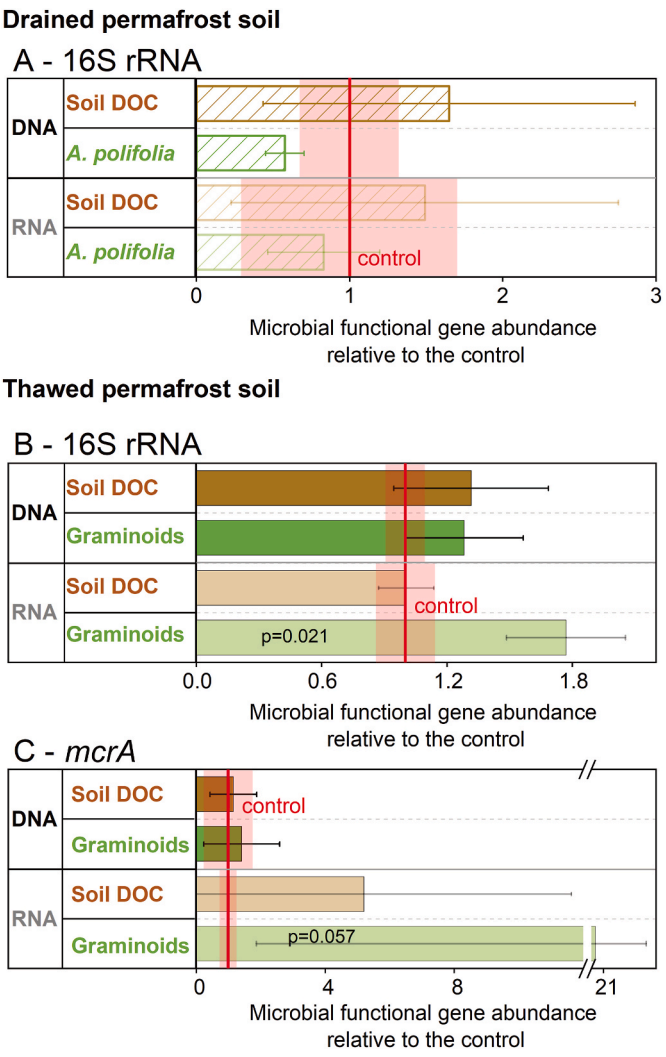

Fig. 5. Microbial functional gene and transcript copy numbers (16S rRNA, *mcrA*) of drained and thawed permafrost soils from Stordalen mire, Abisko, Sweden exposed to different carbon substrates. (A, B) DNA- and RNA-based 16S rRNA copy numbers at day 1 for drained and thawed soil after OC addition relative to the control (red line). (C) Numbers of *mcrA* copies and transcripts at day 1 for the thawed permafrost soil. The red control line is set to 1; values > 1 indicate increases and <1 indicate decreases relative to the control. The shaded red area is the standard error of the control. Mean ± SE, n = 3. P-values, relative to the control are included when $p < 0.1$, all p-values presented in Table S14. The full time-series are in Fig. S4 and Table S13. (For interpretation of the references to colour in this figure legend, the reader is referred to the Web version of this article.)

copies here are considered a proxy for total microbial numbers, 16S rRNA transcript copies serve to proxy metabolically active microorganisms.

Adding thawed permafrost soil with soil DOC and graminoid exudates did not affect 16S rRNA gene copy numbers compared to the control after day 1 (Fig. 5B). Potential microbial activity, indicated by 16S rRNA transcript numbers, was significantly increased by graminoid exudates after day 1. Across matched sampling times, CH_4 fluxes were highest when *mcrA* transcripts were elevated in thawed permafrost soils (day 1; Figs. 4D and 5C), whereas CO_2 fluxes tracked 16S rRNA transcript abundance in both soils (Fig. 4A and B; Fig. 5A and B).

Adding thawed permafrost soil DOC did not increase *mcrA* gene copy and transcript numbers initially compared to the control (Fig. 5C). Graminoid OC also did not increase *mcrA* gene copies, but the *mcrA* transcript response increased 18-fold after 1 day in thawed permafrost soils, coinciding with the early CH_4 peak (Fig. 4D). In both soils, *pmoA* was not detected at any time point, indicating low methanotroph abundance/activity under the incubation conditions.

3.5. *Water-extractable soil geochemistry and solid-phase Fe dynamics during incubation*

Unless stated otherwise, DOC, NH_4^+, NO_3^-, and aqueous Fe refer to concentrations measured in water extracts/supernatants and are used as porewater geochemical proxies, whereas 0.5 M HCl–extractable Fe(II)/Fe_{tot} represents an operationally defined solid-phase Fe pool.

DOC in the drained permafrost soil control was 27.9 ± 3.7 mg L^{-1} at day 0 (Table S15). Neither addition of drained permafrost soil DOC nor *A. polifolia* exudates caused significant changes in DOC relative to the control (Fig. 6A–Table S16). $SUVA_{254}$-based aromaticity of the drained control was 3.2 L mg $^1m^{-1}$ in the first two days of incubation (Fig. 6C). Adding *A. polifolia* exudates insignificantly decreased the aromaticity by 10% relative to the control but significantly ($p = 0.035$) relative to the drained permafrost soil DOC treatment. Solid phase Fe in the drained control was at 0.09 ± 0.02 μM g^{-1} soil during the pre-incubation (Fig. S5) and remained steady during incubation. No changes were found stemming from the OC additions.

The ratio of solid phase 0.5 M HCl extractable Fe(II)/Fe_{tot} was 0.12 ± 0.01 in the pre-incubation and did not change in the drained control soil over time (Fig. 6E). Adding drained permafrost soil DOC to the drained permafrost soil tended to increase the Fe(II)/Fe_{tot} ratio. *A. polifolia* exudates significantly increased the Fe(II)/Fe_{tot} ratio by 33%. After three days of incubation, the Fe(II)/Fe_{tot} ratios were the same among treatments which persisted until the end of the experiment (Fig. S5B).

The initial DOC in the thawed permafrost soil for the control was 44.7 ± 4.5 mg L^{-1} (Table S15). During the pre-incubation, DOC in the control increased by 27% (Fig. 6B) to 56.2 ± 8.1 mg L^{-1}, then remained stable throughout incubation thereafter (Fig. 6B). Under OC addition, after the pre-incubation, DOC increased by 39% (graminoid exudates) and by 42% (soil DOC). Following the thawed permafrost soil DOC addition, DOC remained stable above the control. Meanwhile, the DOC in thawed permafrost soils spiked with graminoid exudates consistently decreased during incubation. It was significantly lower than any other treatment ($p < 0.01$). The observed decreased DOC exceeded the amount of added root-exudate-derived OC (15% added) and reached the DOC content present in the pre-incubation. The aromaticity of the thawed permafrost soil control was 5.1 L $mg^{-1}m^{-1}$ at the beginning of the experiment (Fig. 6D). Addition of thawed permafrost soil DOC significantly increased aromaticity by 10% ($p = 0.005$), and graminoid OC significantly decreased aromaticity by 20% ($p = 0.005$) after 4-7 days. After 40 days, graminoid OC weakly but still significantly ($p = 0.005$) decreased aromaticity while significant differences caused by thawed permafrost soil DOC did not persist to the end of incubation (Fig. S8, Table S16).

Aqueous Fe_{tot} in the thawed control started at 10.9 ± 0.8 μM g^{-1} soil in the pre-incubation (Fig. 6F). Aqueous Fe_{tot} did not differ under thawed permafrost soil DOC addition, though addition of graminoid exudates significantly increased aqueous Fe by 101% ($p < 0.001$). In all treatments, aqueous Fe decreased after day 4, with the strongest decrease for the graminoid exudates (Fig. S5). At the end of the incubation, the aqueous Fe was the same in control and thawed permafrost soil aqueous Fe but was still significantly increased for the soil spiked with graminoid exudates ($p < 0.001$) (Fig. S5).

Water-extracted ammonium amounted to 1.3 ± 0.2 μM g^{-1} dry soil in the drained permafrost soil prior to the pre-incubation phase. In the control treatment, it remained unchanged at 1.4 ± 0.1 μM g^{-1} dry soil during incubation (Fig. S6). Only the addition of *A. polifolia* exudates tended to increase porewater ammonium by 12% ($p = 0.061$) on day 0 and later remained constant relative to the control.

Porewater nitrate in the drained permafrost soil was 1.34 ± 0.05 μM

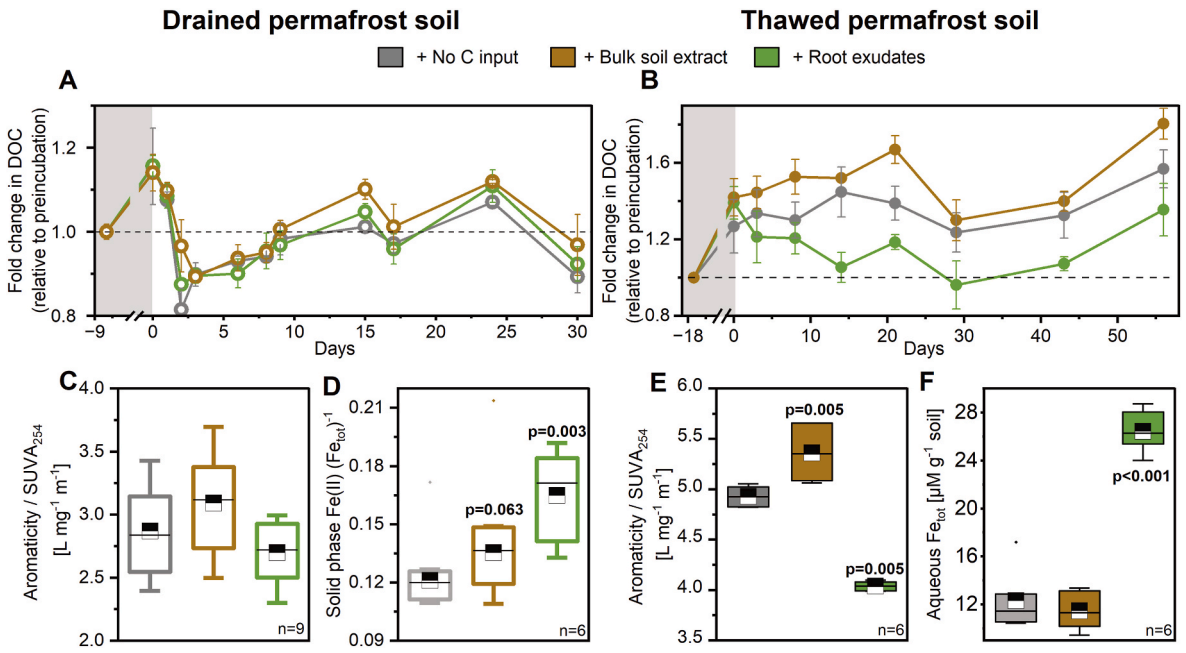

Fig. 6. Porewater organic carbon and Fe dynamics of drained and thawed soils, obtained from a permafrost thaw profile in Stordalen mire, Abisko, Sweden exposed to different carbon substrates. Time-resolved dissolved organic carbon of the (A) drained soil and the (B) thawed soil during incubation. Grey shading depicts the pre-incubation period. Mean ± 1SD, n = 3. Aromaticity is given for the timeframe where OC addition affected aromaticity: (C) 0-2 days in the drained and for the thawed soil (D) for 4-7 days. (E) 0.5 M HCl extractable (solid phase) Fe(II) $(Fe_{tot})^{-1}$ in the drained soil for 0-2 days and (F) aqueous Fe_{tot} in the thawed soil for 0-4 days. Significant differences of the treatment relative to the control are indicated with p-values above plots when $p < 0.1$. Concentrations for DOC can be found in Table S15 and all p-values in Table S16, time-resolved Fe concentrations in Fig. S6 and p-values in Table S18, for aromaticity in Fig. S8 and p-values in Table S17.

g^{-1} dry soil prior to the pre-incubation phase (Fig. S6). During the incubation, nitrate in the control treatment increased to 1.48 ± 0.07 µM g^{-1} dry soil. After a slight decrease to 1.36 ± 0.02 µM g^{-1} dry soil after 2 days, porewater nitrate increased to 1.96 ± 0.1 µM g^{-1} dry soil in the drained permafrost soil control by the end of incubation. Addition of drained permafrost soil DOC did not alter porewater nitrate compared to the control. Adding *A. polifolia* exudates increased porewater nitrate to 1.56 ± 0.03 µM g^{-1} dry soil directly after substrate addition, which decreased to 1.44 ± 0.01 µM g^{-1} dry soil the day after substrate addition and subsequently was not different from the other treatments.

Porewater nitrate in the thawed permafrost soil was 0.22 ± 0.02 µM g^{-1} dry soil prior to the pre-incubation in the control treatment and decreased to 0 after 14 days (Fig. S6). Subsequently, it slightly increased to 0.13 ± 0.02 µM g^{-1} dry soil at the end of the experiment. Thawed permafrost soil DOC addition did not cause differences in porewater nitrate compared to the control. Graminoid exudates increased porewater nitrate to 0.66 ± 0.03 µM g^{-1} dry soil followed by a decrease on days 3, and 14 followed by the same increase as the other treatments thereafter.

4. Discussion

More CH_4 and CO_2 were emitted from vegetated compared to bare thawed permafrost soils in the field (Fig. 3), while emissions were independent of vegetation in the drained permafrost soils. Consistent with this pattern, soil incubations supported that amended graminoid exudates can enhance CH_4 production and CO_2 emissions in thawed, anoxic soils, while shrub exudates triggered only limited responses in drained, oxic soils. Using soil-derived DOC as a baseline allowed us to isolate exudate composition effects within its respective soil context. Metabolite profiles indicate that plant-derived exudates are compositionally distinct from native soil DOC (Fig. 2B). Overall, the direction and magnitude of RPE reflected interactions between plant-derived metabolites and soil properties (hydrology-based anoxic/oxic conditions, pH, Fe and SOC accessibility, and DOC chemistry) (AminiTabrizi et al., 2020; Wilson et al., 2022; Wang and Kuzyakov, 2024), supporting recent evidence that RPE in permafrost soils is strongly context-dependent (Wild et al., 2023; Friggens et al., 2025).

Extending incubations captured longer-term effects on C cycling including priming. In thawed permafrost soils, graminoid exudates significantly increased CO_2 priming (+13%) compared to the control, whereas drained permafrost soils showed no significant priming effects (Fig. S8). Together, these results indicate sustained SOC stimulation in thawed soils following graminoid exudate inputs, but limited priming in drained soils under shrub exudation. The following sections therefore examine (i) the graminoid exudate–thawed permafrost soil system and (ii) the *A. polifolia* exudate–drained permafrost soil system in detail. Although thawed soils originate from the drained palsa, thaw transforms them into a distinct geochemical environment. Therefore, we discuss the two systems separately in terms of their capacity to process plant-specific exudate inputs. Given the ~30 m sampling distance, some spatial variability in initial soil properties cannot be excluded. However, the rapid thaw dynamics in this peatland suggest that the observed shifts predominantly reflect thaw-induced transformation rather than pre-existing differences. Finally, because we tested one shrub representative *(A. polifolia)* and a graminoid functional group *(Eriophorum ssp./ Carex ssp.)* using hydroponically collected exudates in microcosms, responses may differ across species, seasons, and in situ rhizosphere conditions, highlighting priorities for future work to broaden species coverage and integrate microcosms with ecosystem-scale observations.

4.1. Graminoid exudates elicit strong biogeochemical responses in thawed permafrost soil

The anoxic thawed permafrost soil, with its pH of 5.4 ± 0.2, high MAOC content, and presence of dissolved fatty acids, proved responsive to fresh C input in graminoid vegetated field plots (Fig. 3) as well as in the laboratory (Fig. 4). Anoxic soil conditions likely caused energetic

limitations on the rates of lower-energetic anaerobic metabolisms like Fe (III) reduction due to a relative accumulation of reduced and complex C compounds, as previously observed (Naughton et al., 2021) and theoretically rationalized (LaRowe and Van Cappellen, 2011; Sutton-Grier et al., 2011). This is indicated here by a low $NOSC_m$ in the thawed permafrost soil of −1.7 along with a relative enrichment of less decomposable compounds like hydrobenzoic acid and galactitol (Fig. 2B).

Graminoid exudates ($NOSC_m = -0.5$) likely increased the thermodynamic feasibility of Fe(III) reduction (Keiluweit et al., 2016; Gunina and Kuzyakov, 2022), supporting the idea that fresh root-derived C can provide the energy needed to overcome energetic constraints and unlock nutrients from complex SOC pools (Friggens et al., 2025). At the same time, graminoid-obtained acids and sugars reduced dissolved OC aromaticity and mobilized Fe, consistent with exudate-driven complexation/acidification promoting mineral dissolution and priming (Keiluweit et al., 2015). The rise in aqueous Fe(II) further points to active Fe(III) reduction, indicating a functionally diverse community that includes Fe-cyclers, fermenters, and methanogens, as reported for thawed permafrost soils (Woodcroft et al., 2018; AminiTabrizi et al., 2020; Monteux et al., 2020; Patzner et al., 2022). Such metabolically flexible communities are consistent with evidence that positive rhizosphere priming in permafrost soils can be driven by microorganisms using fresh C inputs to fuel extracellular enzyme production and accelerate SOC decomposition (Friggens et al., 2025).

Consistent with these mechanisms, graminoid exudates rapidly increased microbial activity, as shown by a 51% increase in CO_2 emissions relative to the control and elevated 16S rRNA transcript copy numbers shortly after addition. This is consistent with the rhizosphere priming theory and meta-analyses (Huo et al., 2017; Kuzyakov and Razavi, 2019). A concurrent decrease in DOC (Table S15) suggested microbial utilization of both introduced and native SOC, as expected when exudates mobilize MAOC and stimulate co-metabolism (Keiluweit et al., 2015; Jilling et al., 2021). Together, these responses suggest that graminoid exudates did not only stimulate uptake of plant-derived C but also promoted decomposition of native SOC resulting in an RPE. RPE diverged by substrate type with graminoid exudates inducing a positive RPE (+13%), while thawed permafrost soil OC led to a negative priming effect (−12%) (Fig. S8). This substrate-dependent shift in priming direction is supported by recent evidence that priming responses in cold soils depend on the balance between energy supply and nutrient demand rather than C input alone (Bernard et al., 2022; Friggens et al., 2025). Accordingly, soil DOC addition may have shifted microbial metabolism toward the more accessible added OC substrates, whereas graminoid exudates actively stimulated native SOC decomposition.

Exudate-specific initial stimulation of methanogens was evidenced by an 83% and 15% increase in CH_4 emissions relative to the control and bulk soil DOC, respectively (Fig. 4D). This is likely caused by increased methanogen activity based on *mcrA* gene transcripts (Fig. 5C). Graminoid exudates supplied labile sugars and organic acids that fueled fermentation and provided acetate and related substrates, consistent with acetoclastic methanogenesis (Bellisario et al., 1999; Ström et al., 2012) as a key pathway in fully thawed permafrost soils (AminiTabrizi et al., 2020). Because of the stronger warming potential of CH_4, this methanogenic stimulation increased net CO_2-eq emissions during the early phase of incubation (Fig. 4E).

However, the response to graminoid exudates was not constant. After the initial CH_4 stimulation, CH_4 emissions declined below the control by the end of incubation (Fig. S3F). This transition is consistent with rapid depletion of fermentable substrates coupled with mobilization of alternative electron acceptors by graminoid carboxylates, evidenced by a transient aqueous Fe pulse and nitrate dynamics (Fig. 6F; Fig. S6). Under graminoid exudates, cumulative CH_4 negatively correlated with aqueous Fe_{tot} and NO_3^- ($R^2 = 0.73$ and 0.89; Fig. S9). These patterns are consistent with processes known to suppress methanogenesis and can support anaerobic CH_4 oxidation (Shi et al., 2022; Voggenreiter et al., 2025).

Under natural conditions, continuous graminoid exudation during active photosynthesis in thawed fen soils would likely sustain rhizosphere priming and associated reduction processes over longer time frames than captured by a single-pulse addition. MAOC-derived and exudate-derived carboxylic acids (e.g., malic and propionic acid detected in graminoid exudates) could further promote mineral dissolution and Fe(III) reduction, reinforcing these pathways (Kostka et al., 1999; Liang et al., 2024). Consequently, rhizosphere priming of methanogenesis could be an underexplored, yet climate-relevant, biogeochemical interaction in the Arctic terrestrial climate feedback. Finally, despite field-sampling, plants incubated under laboratory conditions may experience physiological stress, potentially altering the quantity or composition of exudates relative to undisturbed conditions. Therefore, while the exact magnitude of the observed CH_4 emissions and priming effects might differ in situ, the overall trends and underlying biogeochemical processes are likely comparable.

4.2. *A. polifolia* exudates induce small effects in drained permafrost soil

In drained, oxic permafrost soil, low pH and phenolic-rich DOC (higher $SUVA_{(254)}$) likely constrain microbial growth and enzymatic access to SOC, while abundant, readily oxidizable POC and energetically efficient aerobic metabolisms reduce the advantage of additional labile inputs (Table S5; Fig. 2; Fig. 6A–C). Consistent with this mechanistic constraint, *A. polifolia* exudate additions produced only weak geochemical and microbial responses: *A. polifolia* exudates, amino-acid-biased and relatively low in sugars, primarily shifted N cycling rather than inducing broad SOC priming, as reflected by a modest, transient NH_4^+ increase (day 0; +12%, $p = 0.061$) (Fig. S6), weak 16S rRNA gene/transcript responses (Fig. 5A), stable Fe pools ($Fe(II)/Fe_{tot}$ and solid Fe; Fig. 5E; Fig. S5), and minimal effects on CO_2 with negligible CH_4 under oxic conditions (Fig. 4A; Fig. S3E). These laboratory constraints align with field chamber measurements showing little vegetation effect at drained sites (Fig. 3). Several factors might contribute to this resistance: the soil's low pH, high SOC content, a substantial fraction of POC, and a DOC signature rich in aromatic and phenolic compounds, as observed here and in other studies (Wild et al., 2023; Wang and Kuzyakov, 2024; Friggens et al., 2025) (Table S5, Fig. 2).

Aerobic degradation of soil organic matter should allow oxygen to oxidize compounds across the full range of $NOSC_m$ values. Thus, in oxic soils, already rich in readily available POC, with energetically efficient aerobic metabolisms, the addition of *A. polifolia* exudates with a $NOSC_m$ of −0.5 might have a minor impact on mineralization rates (Keiluweit et al., 2016; Wilson et al., 2022) (Fig. 2A), given reduced need for microbes to utilize more resistant C sources when fresh OC is added (Li et al., 2018). At the same time, the phenolic character of drained-soil DOC may actively suppress decomposition: phenolic compounds such as hydroquinone, salicylic acid, and hydroxybenzoic acid, known for their role as a “slow C pool” and toxic and/or inhibitory effects on various microbes can impede microbial processing (Freeman et al., 2004; Fudyma et al., 2019; Hough et al., 2020; Wilson et al., 2022) (Fig. 2B). Although *A. polifolia* exudates are compositionally distinct from soil DOC (Fig. 2), these constraints were not overcome, consistent with the stable Fe pools and minor microbial responses noted above. Field CO_2 fluxes at drained sites additionally include autotrophic root respiration, whereas microcosms capture only microbial decomposition of added exudates and native SOC, explaining differences in absolute CO_2 magnitudes but not the consistently weak response.

The acidic soil pH creates unfavourable conditions for most soil microbes (AminiTabrizi et al., 2020; Wang and Kuzyakov, 2024), consistent with low 16S rRNA gene copy numbers (Fig. 5A). Lichens and mosses that cover drained permafrost soil (Malmer et al., 2005; Hough et al., 2020) release acidifying compounds that lower substrate quality and diversity (AminiTabrizi et al., 2020). Lower microbial diversity and fewer cells in drained vs thawed permafrost soil have been observed

before (Woodcroft et al., 2018). Together, low pH and a chemically complex C pool may favor substrate-specialized communities over generalists (AminiTabrizi et al., 2020; Chen et al., 2020; Zhou et al., 2020).

A. polifolia exudates with low C/N ratio, characterized by low sugar but high amino acid concentrations (Fig. 2), suggest a resource strategy that promotes N turnover more than rapid C-driven microbial expansion, as evidenced by low CO_2 release and minor changes in DOC concentrations (Table S5, Figs. 2B–4A and 6A). The dominance of various amino acids over sugars and the relative enrichment of certain ligands like citric acids might stimulate a specialized soil community, as observed before (Landi et al., 2006; Moe, 2013). The slight NH_4^+ increase following *A. polifolia* additions may therefore reflect selective stimulation of N-mineralizing taxa rather than enhanced SOC decomposition (Lu et al., 2011) which has been proposed as particularly relevant in high C/N systems (Craine et al., 2007), as here with a C/N of 125 (Table S5). This is also consistent with studies showing that this strategy reduces overall SOC priming by decreasing the need for soil organic matter degrading enzymes (Rousk et al., 2016; Michel et al., 2023).

Overall, the consistently limited response in microbial activity and GHG emissions observed in both our laboratory incubations (Figs. 4–6) and field observations (Fig. 3) underscores the ecological relevance. This indicates that microbial processes in drained permafrost soil may be constrained by substrate quality and chemical composition, restricting the ecological impact of shrub exudation. Similar limited responses in drained, acidic peatlands have been reported elsewhere (Malmer et al., 2005; Woodcroft et al., 2018; Hough et al., 2020). However, caution is needed when extrapolating these observations to broader field conditions.

4.3. Higher CO_2-equivalent greenhouse gas emissions by root exudates in thawed than drained permafrost soil

Our results show the importance of considering vegetation shifts following thaw and the associated changes in plant species-specific exudation profiles in evaluating the impact of plant-soil interactions on GHG emissions from and the radiative balance of permafrost ecosystems.

It must be noted that ecosystem changes upon thaw are diverse, and we only investigated responses in one representative site for soil inundation upon thaw. Field exudation is continuous and seasonally variable, whereas our laboratory additions were pulsed at an environmentally representative concentration. Thus, short-term effects likely approximate the lower-upper range of seasonal dynamics without fully representing them. In addition, dissolved analytes were measured as water-extractable proxies, and 0.5 M HCl Fe represents an operational solid-phase pool, which constrains direct comparison to in situ porewater and minerals.

Graminoid exudates increased the net CO_2-eq emission of thawed permafrost soil by 69% relative to the control over the first 5 days in laboratory incubations, compared to a 9% increase in net CO_2-eq emissions from drained oxic microcosms amended with *A. polifolia* exudates (Fig. 4E). This contrast was driven largely by a stronger CH_4 contribution to CO_2-eq in thawed soils, consistent with recent evidence that CH_4 emissions can dominate the forcing outcomes in permafrost-region budgets (Hugelius et al., 2024). Overall, thawed permafrost soil spiked with graminoid exudates showed an approximately 160% higher net CO_2-eq emission than the drained permafrost soil spiked with *A. polifolia* exudates (Fig. 4E). This is due to a stepwise increase: even without added OC, the net CO_2-eq emission increased by 40% in the untreated control soil upon thaw (within the first five days, Fig. 4E). When soils were treated with their own soil DOC, the net CO_2-eq emission increased by 77% from drained to thawed conditions. This indicates that thawed permafrost soil has a stronger stimulation potential than drained permafrost soil, even when the added C is relatively high in aromaticity and has a negative NOSC. Thus, thaw-driven changes in soil redox/chemistry and plant-specific inputs jointly amplify net CO_2-eq emissions, consistent with prior observations that thaw and wetting can shift systems toward higher CH_4-driven climate forcing (Hodgkins et al., 2014; McCalley et al., 2014).

Some Earth System Model projections suggest that ~80% of near-surface permafrost could disappear by 2100 (Pörtner et al., 2019; Peng et al., 2023). Compared to the global average temperature, the 3-4-fold amplified increase in atmospheric temperatures in Arctic ecosystems (Rantanen et al., 2022) can have cascading effects in further changing plant traits (Christensen et al., 2004; Malmer et al., 2005; Blume-Werry et al., 2019). This might include a higher amount of root exudation, deeper growing graminoid roots reaching new C pools, longer growing seasons (Wolkovich et al., 2012; IPCC et al., 2022) and warming-induced increases in soil microbiome activity (Jorgenson et al., 2001; Malmer et al., 2005; Johansson et al., 2006; Blume-Werry et al., 2019). Recent field evidence links thaw-stage vegetation shifts (often toward graminoids) with strong increases in CH_4 emissions (Cox et al., 2024), consistent with the mechanisms identified here. It is therefore urgent to resolve how thaw-driven hydrologic change and vegetation transitions interact with rhizosphere priming of CO_2 and CH_4 production to improve estimates of the magnitude and gas partitioning of the Arctic terrestrial climate feedback.

5. Conclusions

This study directly linked field observations of GHG emissions with controlled laboratory experiments to highlight that plant species-specific root exudation can shape Arctic permafrost C feedback on top of known hydrological impacts on GHG emissions. The findings of this study further explain the field-derived GHG emission data for the thawing permafrost peatland in Stordalen mire near Abisko, Sweden, and may be transferable to other Arctic regions. A key innovation is the field-lab framework combined with a soil context baseline, which allows attributing GHG responses to the composition of exudates rather than to C addition alone. Our site-specific design (one mire, one shrub and graminoid representative, ~30 m separation of soil cores) and hydroponic exudate collection limit generalization, yet the direction and magnitude of graminoid-driven CH_4 enhancement under anoxia were consistent across field and lab observations. Given the rapid shifts in soil habitats and plant communities driven by permafrost thaw, integrating laboratory insights with field-scale observations remains essential for accurately predicting future changes in Arctic GHG emissions. Thus, not only hydrologic state but also plant-specific exudate composition governs net GHG balance, with graminoid rhizospheres strengthening methanogenesis and SOC decomposition in thawed peat while shrub rhizospheres remain comparatively muted in drained soils.

CRediT authorship contribution statement

Marie Mollenkopf: Writing – review & editing, Writing – original draft, Visualization, Validation, Project administration, Methodology, Investigation, Funding acquisition, Formal analysis, Data curation, Conceptualization. **Sylvain Monteux:** Writing – review & editing, Validation. **Ellen Dorrepaal:** Writing – review & editing. **Birgit Wild:** Writing – review & editing, Conceptualization. **Joachim Kilian:** Writing – review & editing, Methodology, Data curation. **Mark Stahl:** Writing – review & editing, Data curation. **Andreas Kappler:** Writing – review & editing, Supervision, Project administration, Methodology, Conceptualization. **E. Marie Muehe:** Writing – review & editing, Writing – original draft, Validation, Supervision, Resources, Project administration, Investigation, Funding acquisition, Conceptualization.

Declaration of competing interest

The authors declare that they have no known competing financial interests or personal relationships that could have appeared to influence

the work reported in this paper.

Acknowledgements

We appreciate and are thankful for the support we experienced from the Swedish Polar Research Secretariat and SITES at the Abisko Research Station (Abisko, Sweden). The authors would like to thank ICOS Sweden for providing meteorological data. We thank A. Gloeckle, L. Haas, K. Lenge, S. Wild, D. Buchner, C. Banfield, F. Schädler, and the Geomicrobiology group members for the help in the laboratory. We thank P. Joshi, E. Voggenreiter, K. Wunsch, and A. Chauhan for the field assistance and the discussions in the permafrost meeting. We are grateful to C. Schmidt for a first draft of the proposal giving good scientific direction. We further acknowledge financial and infrastructural support by the Deutsche Forschungsgemeinschaft (DFG, German Research Foundation) and proposal number 465839667. E.M.M acknowledges the Helmholtz Young Investigator Grant RhizoThreats. B.W. additionally acknowledges ERC StG PRIMETIME (grant number 101039588) and the Swedish Research Council VR (grant number 2022-03940). We acknowledge biorender.com, which we used for preparation of schematics including the graphical abstract.

Appendix A. Supplementary data

Supplementary data to this article can be found online at https://doi.org/10.1016/j.soilbio.2026.110110.

References

Åkerman, H.J., Johansson, M., 2008. Thawing permafrost and thicker active layers in sub-arctic Sweden. Permafrost and Periglacial Processes 19, 279–292.
AminiTabrizi, R., Wilson, R.M., Fudyma, J.D., Hodgkins, S.B., Heyman, H.M., Rich, V.I., Saleska, S.R., Chanton, J.P., Tfaily, M.M., 2020. Controls on soil organic matter degradation and subsequent greenhouse gas emissions across a permafrost thaw gradient in northern Sweden. Frontiers in Earth Science 8, 557961.
Apprill, A., McNally, S., Parsons, R., Weber, L., 2015. Minor revision to V4 region SSU rRNA 806R gene primer greatly increases detection of SAR11 bacterioplankton. Aquatic Microbial Ecology 75, 129–137.
Avis, C.A., Weaver, A.J., Meissner, K.J., 2011. Reduction in areal extent of high-latitude wetlands in response to permafrost thaw. Nature Geoscience 4, 444–448.
Bäckstrand, K., Crill, P., Jackowicz-Korczynski, M., Mastepanov, M., Christensen, T., Bastviken, D., 2010. Annual carbon gas budget for a subarctic peatland, northern Sweden. Biogeosciences 7, 95–108.
Beilman, D.W., 2001. Plant community and diversity change due to localized permafrost dynamics in bogs of western Canada. Canadian Journal of Botany 79, 983–993.
Bellisario, L., Bubier, J., Moore, T., Chanton, J., 1999. Controls on CH4 emissions from a northern peatland. Global Biogeochemical Cycles 13, 81–91.
Bernard, L., Basile-Doelsch, I., Derrien, D., Fanin, N., Fontaine, S., Guenet, B., Karimi, B., Marsden, C., Maron, P.a., 2022. Advancing the mechanistic understanding of the priming effect on soil organic matter mineralisation. Functional Ecology 36, 1355–1377.
Blume-Werry, G., Milbau, A., Teuber, L.M., Johansson, M., Dorrepaal, E., 2019. Dwelling in the deep–strongly increased root growth and rooting depth enhance plant interactions with thawing permafrost soil. New Phytologist 223, 1328–1339.
Cambardella, C.A., Elliott, E., 1992. Particulate soil organic-matter changes across a grassland cultivation sequence. Soil Science Society of America Journal 56, 777–783.
Chang, R., Liu, S., Chen, L., Li, N., Bing, H., Wang, T., Chen, X., Li, Y., Wang, G., 2021. Soil organic carbon becomes newer under warming at a permafrost site on the Tibetan Plateau. Soil Biology and Biochemistry 152, 108074.
Chen, J., Elsgaard, L., van Groenigen, K.J., Olesen, J.E., Liang, Z., Jiang, Y., Laerke, P.E., Zhang, Y., Luo, Y., Hungate, B.A., Sinsabaugh, R.L., Jorgensen, U., 2020. Soil carbon loss with warming: new evidence from carbon-degrading enzymes. Global Change Biology 26, 1944–1952.
Christensen, T.R., Johansson, T., Åkerman, H.J., Mastepanov, M., Malmer, N., Friborg, T., Crill, P., Svensson, B.H., 2004. Thawing sub-arctic permafrost: effects on vegetation and methane emissions. Geophysical Research Letters 31.
Cotrufo, M.F., Ranalli, M.G., Haddix, M.L., Six, J., Lugato, E., 2019. Soil carbon storage informed by particulate and mineral-associated organic matter. Nature Geoscience 12, 989–994.
Cox, W.D., Dieleman, C., Douglas, T.A., Kane, E.S., Neumann, R.B., Euskirchen, E.S., Turetsky, M.R., 2024. Plant Community Shifts as Early Indicators of Abrupt Permafrost Thaw and Associated Carbon Release in an Interior Alaskan Peatland. Authorea Preprints.
Craine, J.M., Morrow, C., Fierer, N., 2007. Microbial nitrogen limitation increases decomposition. Ecology 88, 2105–2113.
Fewster, R.E., Morris, P.J., Ivanovic, R.F., Swindles, G.T., Peregon, A.M., Smith, C.J., 2022. Imminent loss of climate space for permafrost peatlands in Europe and Western Siberia. Nature Climate Change 12, 373–379.
Freeman, C., Ostle, N., Fenner, N., Kang, H., 2004. A regulatory role for phenol oxidase during decomposition in peatlands. Soil Biology and Biochemistry 36, 1663–1667.
Friedlingstein, P., 2020. Global Carbon Budgets: Determining Limits on Fossil Fuel Emissions.
Friggens, N.L., Hugelius, G., Kokelj, S.V., Murton, J.B., Phoenix, G.K., Hartley, I.P., 2025. Positive rhizosphere priming accelerates carbon release from permafrost soils. Nature Communications 16, 3576.
Fudyma, J.D., Lyon, J., AminiTabrizi, R., Gieschen, H., Chu, R.K., Hoyt, D.W., Kyle, J.E., Toyoda, J., Tolic, N., Heyman, H.M., Hess, N.J., Metz, T.O., Tfaily, M.M., 2019. Untargeted metabolomic profiling of Sphagnum fallax reveals novel antimicrobial metabolites. Plant Direct 3, e00179.
Gee, G.W., Or, D., 2002. 2.4 Particle-size analysis. Methods of soil analysis: Part 4 physical methods. In: , 5, pp. 255–293.
Gunina, A., Kuzyakov, Y., 2022. From energy to (soil organic) matter. Global Change Biology 28, 2169–2182.
He, M., Li, Q., Chen, L., Qin, S., Kuzyakov, Y., Liu, Y., Zhang, D., Feng, X., Kou, D., Wu, T., 2023. Priming effect stimulates carbon release from thawed permafrost. Global Change Biology 29, 4638–4651.
Heijmans, M.M., Magnússon, R.Í., Lara, M.J., Frost, G.V., Myers-Smith, I.H., van Huissteden, J., Jorgenson, M.T., Fedorov, A.N., Epstein, H.E., Lawrence, D.M., 2022. Tundra vegetation change and impacts on permafrost. Nature Reviews Earth & Environment 3, 68–84.
Hodgkins, S.B., Tfaily, M.M., McCalley, C.K., Logan, T.A., Crill, P.M., Saleska, S.R., Rich, V.I., Chanton, J.P., 2014. Changes in peat chemistry associated with permafrost thaw increase greenhouse gas production. Proceedings of the National Academy of Sciences of the U S A 111, 5819–5824.
Hough, M., McClure, A., Bolduc, B., Dorrepaal, E., Saleska, S., Klepac-Ceraj, V., Rich, V., 2020. Biotic and environmental drivers of plant microbiomes across a permafrost thaw gradient. Frontiers in Microbiology 11, 796.
Hugelius, G., Ramage, J., Burke, E., Chatterjee, A., Smallman, T.L., Aalto, T., Bastos, A., Biasi, C., Canadell, J.G., Chandra, N., 2024. Permafrost region greenhouse gas budgets suggest a weak CO2 sink and CH4 and N2O sources, but magnitudes differ between top-down and bottom-up methods. Global Biogeochemical Cycles 38 e2023GB007969.
Huo, C., Luo, Y., Cheng, W., 2017. Rhizosphere priming effect: a meta-analysis. Soil Biology and Biochemistry 111, 78–84.
Icos, Sweden, Lundin, E., Rinne, J., 2021a. Ecosystem meteo time series (ICOS Sweden) from Abisko-Stordalen Palsa Bog, 2016-12-31–2017-12-31, Swedish national network. https://hdl.handle.net/11676/RsEekosuKKJQ_DfhhFdEQKOa.
Icos, Sweden, Lundin, E., Rinne, J., 2021b. Ecosystem meteo time series (ICOS Sweden) from Abisko-Stordalen Palsa Bog, 2017-12-31–2018-12-31, Swedish national network. https://hdl.handle.net/11676/CLkw56hpo6p_Zy59eBnn5hY2.
Icos, Sweden, Lundin, E., Rinne, J., 2021c. Ecosystem meteo time series (ICOS Sweden) from Abisko-Stordalen Palsa Bog, 2018-12-31–2019-12-31, Swedish national network. https://hdl.handle.net/11676/OxWpxiic7m5hvaErFHBzTS1q.
Icos, Sweden, Lundin, E., Rinne, J., 2021d. Ecosystem meteo time series (ICOS Sweden) from Abisko-Stordalen Palsa Bog, 2019-12-31–2020-12-31, Swedish national network. https://hdl.handle.net/11676/pyzzIVYElaSZedqHz2DyjjWe.
Icos, Sweden, Lundin, E., Rinne, J., 2022. Ecosystem meteo time series (ICOS Sweden) from Abisko-Stordalen Palsa Bog, 2020-12-31–2021-12-31, Swedish national network. https://hdl.handle.net/11676/xWk7ApA26gjb9o3hT0y98cCS.
Icos, Sweden, Lundin, E., Rinne, J., 2023. Ecosystem meteo time series (ICOS Sweden) from Abisko-Stordalen Palsa Bog, 2021-12-31–2022-12-31, Swedish national network. https://hdl.handle.net/11676/qk6Tpkpn5vkR4n5RvJRZKF-G.
IPCC, 2022. In: Pörtner, H.-O., D.C.R., Tignor, M., Poloczanska, E.S., Mintenbeck, K., Alegría, A., Craig, M., Langsdorf, S., Löschke, S., Möller, V., Okem, A., Rama, B. (Eds.), Climate Change 2022: Impacts, Adaptation, and Vulnerability. Contribution of Working Group II to the Sixth Assessment Report of the Intergovernmental Panel on Climate Change.
IPCC, 2023. Summary for Policymakers, Climate Change 2021 – the Physical Science Basis. Cambridge University Press, Cambridge, United Kingdom and New York, NY, US, pp. 3–32.
Iversen, C.M., Sloan, V.L., Sullivan, P.F., Euskirchen, E.S., McGuire, A.D., Norby, R.J., Walker, A.P., Warren, J.M., Wullschleger, S.D., 2015. The unseen iceberg: plant roots in arctic tundra. New Phytologist 205, 34–58.
Jean Le Mer, P.R., 2001. Production, oxidation, emission and consumption of methane by soils: a review. European Journal of Soil Biology 37, 25–50.
Jilling, A., Keiluweit, M., Gutknecht, J.L., Grandy, A.S., 2021. Priming mechanisms providing plants and microbes access to mineral-associated organic matter. Soil Biology and Biochemistry 158, 108265.
Joabsson, A., Christensen, T.R., Wallen, B., 1999. Vascular plant controls on methane emissions from northern peatforming wetlands. Trends in Ecology & Evolution 14, 385–388.
Johansson, T., Malmer, N., Crill, P.M., Friborg, T., Åkerman, J.H., Mastepanov, M., Christensen, T.R., 2006. Decadal vegetation changes in a northern peatland, greenhouse gas fluxes and net radiative forcing. Global Change Biology 12, 2352–2369.
Jones, D.L., Nguyen, C., Finlay, R.D., 2009. Carbon Flow in the Rhizosphere: Carbon Trading at the soil–root Interface. Springer.
Jorgenson, M.T., Racine, C.H., Walters, J.C., Osterkamp, T.E., 2001. Permafrost degradation and ecological changes associated with a warmingclimate in central Alaska. Climatic Change 48, 551–579.

Keiluweit, M., Bougoure, J.J., Nico, P.S., Pett-Ridge, J., Weber, P.K., Kleber, M., 2015. Mineral protection of soil carbon counteracted by root exudates. Nature Climate Change 5, 588–595.
Keiluweit, M., Nico, P.S., Kleber, M., Fendorf, S., 2016. Are oxygen limitations under recognized regulators of organic carbon turnover in upland soils? Biogeochemistry 127, 157–171.
Keuper, F., Wild, B., Kummu, M., Beer, C., Blume-Werry, G., Fontaine, S., Gavazov, K., Gentsch, N., Guggenberger, G., Hugelius, G., 2020. Carbon loss from northern circumpolar permafrost soils amplified by rhizosphere priming. Nature Geoscience 13, 560–565.
Kim, S.Y., Gutierrez, J., Kim, P.J., 2016. Unexpected stimulation of CH4 emissions under continuous no-tillage system in mono-rice paddy soils during cultivation. Geoderma 267, 34–40.
Kostka, J.E., Haefele, E., Viehweger, Ralf, Stucki, J.W., 1999. Respiration and dissolution of Iron(III)-Containing clay minerals by bacteria. Environmental Science and Technology 33, 3127–3133.
Kuzyakov, Y., 2010. Priming effects: interactions between living and dead organic matter. Soil Biology and Biochemistry 42, 1363–1371.
Kuzyakov, Y., Razavi, B.S., 2019. Rhizosphere size and shape: temporal dynamics and spatial stationarity. Soil Biology and Biochemistry 135, 343–360.
Landi, L., Valori, F., Ascher, J., Renella, G., Falchini, L., Nannipieri, P., 2006. Root exudate effects on the bacterial communities, CO2 evolution, nitrogen transformations and ATP content of rhizosphere and bulk soils. Soil Biology and Biochemistry 38, 509–516.
LaRowe, D.E., Van Cappellen, P., 2011. Degradation of natural organic matter: a thermodynamic analysis. Geochimica et Cosmochimica Acta 75, 2030–2042.
Li, H., Bolscher, T., Winnick, M., Tfaily, M.M., Cardon, Z.G., Keiluweit, M., 2021. Simple plant and microbial exudates destabilize mineral-associated organic matter via multiple pathways. Environmental Science and Technology 55, 3389–3398.
Li, J., Ramirez, G.H., Kiani, M., Quideau, S., Smith, E., Janzen, H., Larney, F., Puurveen, D., 2018. Soil organic matter dynamics in long-term temperate agroecosystems: rotation and nutrient addition effects. Canadian Journal of Soil Science 98, 232–245.
Liang, Y., Liu, J., Jin, J., Han, Y., Wei, Z., 2024. Effects of low-molecular-weight organic acids on the transformation and phosphate retention of iron (hydr)oxides. Science of the Total Environment 940, 173667.
Lu, M., Yang, Y., Luo, Y., Fang, C., Zhou, X., Chen, J., Yang, X., Li, B., 2011. Responses of ecosystem nitrogen cycle to nitrogen addition: a meta-analysis. New Phytologist 189, 1040–1050.
Lueders, T., Manefield, M., Friedrich, M.W., 2004. Enhanced sensitivity of DNA- and rRNA-based stable isotope probing by fractionation and quantitative analysis of isopycnic centrifugation gradients. Environmental Microbiology 6, 73–78.
Määttä, T., Malhotra, A., 2024. The hidden roots of wetland methane emissions. Global Change Biology 30 (2), e17127.
Malhotra, A., Brice, D.J., Childs, J., Graham, J.D., Hobbie, E.A., Vander Stel, H., Feron, S. C., Hanson, P.J., Iversen, C.M., 2020. Peatland warming strongly increases fine-root growth. Proceedings of the National Academy of Sciences of the U S A 117, 17627–17634.
Malmer, N., Johansson, T., Olsrud, M., Christensen, T.R., 2005. Vegetation, climatic changes and net carbon sequestration in a North-Scandinavian subarctic mire over 30 years. Global Change Biology 11, 1895–1909.
McCalley, C.K., Woodcroft, B.J., Hodgkins, S.B., Wehr, R.A., Kim, E.H., Mondav, R., Crill, P.M., Chanton, J.P., Rich, V.I., Tyson, G.W., Saleska, S.R., 2014. Methane dynamics regulated by microbial community response to permafrost thaw. Nature 514, 478–481.
Michel, J., Hartley, I.P., Buckeridge, K.M., van Meegen, C., Broyd, R.C., Reinelt, L., Ccahuana Quispe, A.J., Whitaker, J., 2023. Preferential substrate use decreases priming effects in contrasting treeline soils. Biogeochemistry 162, 141–161.
Mishra, U., Hugelius, G., Shelef, E., Yang, Y., Strauss, J., Lupachev, A., Harden, J.W., Jastrow, J.D., Ping, C.L., Riley, W.J., Schuur, E.A.G., Matamala, R., Siewert, M., Nave, L.E., Koven, C.D., Fuchs, M., Palmtag, J., Kuhry, P., Treat, C.C., Zubrzycki, S., Hoffman, F.M., Elberling, B., Camill, P., Veremeeva, A., Orr, A., 2021. Spatial heterogeneity and environmental predictors of permafrost region soil organic carbon stocks. Science Advances 7 eaaz5236.
Moe, L.A., 2013. Amino acids in the rhizosphere: from plants to microbes. American Journal of Botany 100, 1692–1705.
Monteux, S., Keuper, F., Fontaine, S., Gavazov, K., Hallin, S., Juhanson, J., Krab, E.J., Revaillot, S., Verbruggen, E., Walz, J., 2020. Carbon and nitrogen cycling in Yedoma permafrost controlled by microbial functional limitations. Nature Geoscience 13, 794–798.
Monteux, S., Weedon, J.T., Blume-Werry, G., Gavazov, K., Jassey, V.E.J., Johansson, M., Keuper, F., Olid, C., Dorrepaal, E., 2018. Long-term in situ permafrost thaw effects on bacterial communities and potential aerobic respiration. ISME J 12, 2129–2141.
Natali, S.M., Watts, J.D., Rogers, B.M., Potter, S., Ludwig, S.M., Selbmann, A.K., Sullivan, P.F., Abbott, B.W., Arndt, K.A., Birch, L., Bjorkman, M.P., Bloom, A.A., Celis, G., Christensen, T.R., Christiansen, C.T., Commane, R., Cooper, E.J., Crill, P., Czimczik, C., Davydov, S., Du, J., Egan, J.E., Elberling, B., Euskirchen, E.S., Friborg, T., Genet, H., Gockede, M., Goodrich, J.P., Grogan, P., Helbig, M., Jafarov, E.E., Jastrow, J.D., Kalhori, A.A.M., Kim, Y., Kimball, J., Kutzbach, L., Lara, M.J., Larsen, K.S., Lee, B.Y., Liu, Z., Loranty, M.M., Lund, M., Lupascu, M., Madani, N., Malhotra, A., Matamala, R., McFarland, J., McGuire, A.D., Michelsen, A., Minions, C., Oechel, W.C., Olefeldt, D., Parmentier, F.W., Pirk, N., Poulter, B., Quinton, W., Rezanezhad, F., Risk, D., Sachs, T., Schaefer, K., Schmidt, N.M., Schuur, E.A.G., Semenchuk, P.R., Shaver, G., Sonnentag, O., Starr, G., Treat, C.C., Waldrop, M.P., Wang, Y., Welker, J., Wille, C., Xu, X., Zhang, Z., Zhuang, Q., Zona, D., 2019. Large loss of CO(2) in winter observed across the northern permafrost region. Nature Climate Change 9, 852–857.
Naughton, H.R., Keiluweit, M., Tfaily, M.M., Dynes, J.J., Regier, T., Fendorf, S., 2021. Development of energetic and enzymatic limitations on microbial carbon cycling in soils. Biogeochemistry 153, 191–213.
Neubauer, S.C., 2021. Global warming potential is not an ecosystem property. Ecosystems 24, 2079–2089.
Oburger, E., Jones, D.L., 2018. Sampling root exudates–mission impossible? Rhizosphere 6, 116–133.
Parada, A.E., Needham, D.M., Fuhrman, J.A., 2016. Every base matters: assessing small subunit rRNA primers for marine microbiomes with mock communities, time series and global field samples. Environmental Microbiology 18, 1403–1414.
Patzner, M.S., Logan, M., McKenna, A., Young, R.B., Zhou, Z., Joss, H., Mueller, C.W., Hoeschen, C., Scholten, T., Straub, D., 2022. Microbial iron (III) reduction during palsa collapse promotes greenhouse gas emissions before complete permafrost thaw. Communications Earth & Environment 3, 76.
Patzner, M.S., Mueller, C.W., Malusova, M., Baur, M., Nikeleit, V., Scholten, T., Hoeschen, C., Byrne, J.M., Borch, T., Kappler, A., 2020. Iron mineral dissolution releases iron and associated organic carbon during permafrost thaw. Nature Communications 11, 6329.
Peng, X., Zhang, T., Frauenfeld, O.W., Mu, C., Wang, K., Wu, X., Guo, D., Luo, J., Hjort, J., Aalto, J., 2023. Active layer thickness and permafrost area projections for the 21st century. Earth's Future 11 e2023EF003573.
Pörtner, H.-O., Roberts, D.C., Masson-Delmotte, V., Zhai, P., Tignor, M., Poloczanska, E., Weyer, N.M., 2019. The ocean and cryosphere in a changing climate. IPCC special report on the ocean and cryosphere in a changing climate 1155, 10–1017.
Proctor, C., He, Y., 2017. Quantifying root extracts and exudates of sedge and shrub in relation to root morphology. Soil Biology and Biochemistry 114, 168–180.
Quinton, W., Hayashi, M., Chasmer, L., 2011. Permafrost-thaw-induced land-cover change in the Canadian subarctic: implications for water resources. Hydrological Processes 25, 152–158.
Ramirez, J.A., Baird, A.J., Coulthard, T.J., 2016. The effect of pore structure on ebullition from peat. Journal of Geophysical Research: Biogeosciences 121, 1646–1656.
Rantanen, M., Karpechko, A.Y., Lipponen, A., Nordling, K., Hyvärinen, O., Ruosteenoja, K., Vihma, T., Laaksonen, A., 2022. The Arctic has warmed nearly four times faster than the globe since 1979. Communications Earth & Environment 3, 168.
Riedel, T., Biester, H., Dittmar, T., 2012. Molecular fractionation of dissolved organic matter with metal salts. Environmental Science and Technology 46, 4419–4426.
Rousk, K., Michelsen, A., Rousk, J., 2016. Microbial control of soil organic matter mineralization responses to labile carbon in subarctic climate change treatments. Global Change Biology 22, 4150–4161.
Ruser, R., Schilling, R., Steindl, H., Flessa, H., Beese, F., 1998. Soil compaction and fertilization effects on nitrous oxide and methane fluxes in potato fields. Soil Science Society of America Journal 62, 1587–1595.
Saarnio, S., Wittenmayer, L., Merbach, W., 2004. Rhizospheric exudation of Eriophorum vaginatum L.—Potential link to methanogenesis. Plant and Soil 267, 343–355.
Schädel, C., Bader, M.K.-F., Schuur, E.A., Biasi, C., Bracho, R., Čapek, P., De Baets, S., Diáková, K., Ernakovich, J., Estop-Aragones, C., 2016. Potential carbon emissions dominated by carbon dioxide from thawed permafrost soils. Nature Climate Change 6, 950–953.
Schuur, E.A., McGuire, A.D., Schadel, C., Grosse, G., Harden, J.W., Hayes, D.J., Hugelius, G., Koven, C.D., Kuhry, P., Lawrence, D.M., Natali, S.M., Olefeldt, D., Romanovsky, V.E., Schaefer, K., Turetsky, M.R., Treat, C.C., Vonk, J.E., 2015. Climate change and the permafrost carbon feedback. Nature 520, 171–179.
Shi, Y., Ma, Q., Kuzyakov, Y., Sheng, L., Liu, H., Wang, Z., 2022. Nitrite-dependent anaerobic oxidation decreases methane emissions from peatlands. Soil Biology and Biochemistry 169, 108658.
Smith, S.L., O'Neill, H.B., Isaksen, K., Noetzli, J., Romanovsky, V.E., 2022. The changing thermal state of permafrost. Nature Reviews Earth & Environment 3, 10–23.
Stookey, L.L., 1970. Ferrozine—a new spectrophotometric reagent for iron. Analytical Chemistry 42, 779–781.
Street, L.E., Garnett, M.H., Subke, J.A., Baxter, R., Dean, J.F., Wookey, P.A., 2020. Plant carbon allocation drives turnover of old soil organic matter in permafrost tundra soils. Global Change Biology 26, 4559–4571.
Ström, L., Tagesson, T., Mastepanov, M., Christensen, T.R., 2012. Presence of Eriophorum scheuchzeri enhances substrate availability and methane emission in an arctic wetland. Soil Biology and Biochemistry 45, 61–70.
Sutton-Grier, A.E., Keller, J.K., Koch, R., Gilmour, C., Megonigal, J.P., 2011. Electron donors and acceptors influence anaerobic soil organic matter mineralization in tidal marshes. Soil Biology and Biochemistry 43, 1576–1583.
Sutton-Grier, A.E., Megonigal, J.P., 2011. Plant species traits regulate methane production in freshwater wetland soils. Soil Biology and Biochemistry 43, 413–420.
Tarnocai, C., Canadell, J., Schuur, E.A., Kuhry, P., Mazhitova, G., Zimov, S., 2009. Soil organic carbon pools in the northern circumpolar permafrost region. Global Biogeochemical Cycles 23.
Team, R.C., 2024. R: a Language and Environment for Statistical Computing.
Varner, R.K., Crill, P.M., Frolking, S., McCalley, C.K., Burke, S.A., Chanton, J.P., Holmes, M.E., Isogenie Project, C., Saleska, S., Palace, M.W., 2022. Permafrost thaw driven changes in hydrology and vegetation cover increase trace gas emissions and climate forcing in Stordalen mire from 1970 to 2014. Philosophical Transactions of the Royal Society A: Mathematical, Physical and Engineering Sciences 380 (2215).
Verbrigghe, N., Meeran, K., Bahn, M., Fuchslueger, L., Janssens, I.A., Richter, A., Sigurdsson, B.D., Soong, J.L., Vicca, S., 2022. Negative priming of soil organic matter following long-term in situ warming of sub-arctic soils. Geoderma 410, 115652.

Voggenreiter, E., ThomasArrigo, L., Bottaro, M., Kilian, J., Straub, D., Ring-Hrubesh, F., Bryce, C., Stahl, M., Kappler, A., Joshi, P., 2025. Suppression of methanogenesis by microbial reduction of iron-organic carbon associations in fully thawed permafrost soil. Journal of Geophysical Research: Biogeosciences 130 e2024JG008650.

Waldo, N.B., Hunt, B.K., Fadely, E.C., Moran, J.J., Neumann, R.B., 2019. Plant root exudates increase methane emissions through direct and indirect pathways. Biogeochemistry 145, 213–234.

Wang, C., Kuzyakov, Y., 2024. Soil organic matter priming: the pH effects. Global Change Biology 30, e17349.

Wegner, R., Plassmann, M., Sauerland, L., Carter, A., Monteux, S., Oburger, E., Wild, B., 2025. Back to the roots: characterizing root exudates of dominant tundra plants to improve the understanding of plant-soil interactions in a changing arctic. Soil Biology and Biochemistry, 109897.

Wei, L., Zhu, Z., Liu, S., Xiao, M., Wang, J., Deng, Y., Kuzyakov, Y., Wu, J., Ge, T., 2021. Temperature sensitivity (Q10) of stable, primed and easily available organic matter pools during decomposition in paddy soil. Applied Soil Ecology 157, 103752.

Wild, B., Monteux, S., Wendler, B., Hugelius, G., Keuper, F., 2023. Circum-arctic peat soils resist priming by plant-derived compounds. Soil Biology and Biochemistry 180, 109012.

Williams, A., Langridge, H., Straathof, A.L., Muhamadali, H., Hollywood, K.A., Goodacre, R., de Vries, F.T., 2022. Root functional traits explain root exudation rate and composition across a range of grassland species. Journal of Ecology 110, 21–33.

Wilson, R.M., Hough, M.A., Verbeke, B.A., Hodgkins, S.B., IsoGenie, C., Chanton, J.P., Saleska, S.D., Rich, V.I., Tfaily, M.M., 2022. Plant organic matter inputs exert a strong control on soil organic matter decomposition in a thawing permafrost peatland. Science of the Total Environment 820, 152757.

Wolkovich, E.M., Cook, B.I., Allen, J.M., Crimmins, T.M., Betancourt, J.L., Travers, S.E., Pau, S., Regetz, J., Davies, T.J., Kraft, N.J., Ault, T.R., Bolmgren, K., Mazer, S.J., McCabe, G.J., McGill, B.J., Parmesan, C., Salamin, N., Schwartz, M.D., Cleland, E.E., 2012. Warming experiments underpredict plant phenological responses to climate change. Nature 485, 494–497.

Woodcroft, B.J., Singleton, C.M., Boyd, J.A., Evans, P.N., Emerson, J.B., Zayed, A.A.F., Hoelzle, R.D., Lamberton, T.O., McCalley, C.K., Hodgkins, S.B., Wilson, R.M., Purvine, S.O., Nicora, C.D., Li, C., Frolking, S., Chanton, J.P., Crill, P.M., Saleska, S. R., Rich, V.I., Tyson, G.W., 2018. Genome-centric view of carbon processing in thawing permafrost. Nature 560, 49–54.

Xu, Z., Zhou, G., 2011. Responses of photosynthetic capacity to soil moisture gradient in perennial rhizome grass and perennial bunchgrass. BMC Plant Biology 11, 21.

Zhou, L., Zhou, Y., Yao, X., Cai, J., Liu, X., Tang, X., Zhang, Y., Jang, K.S., Jeppesen, E., 2020. Decreasing diversity of rare bacterial subcommunities relates to dissolved organic matter along permafrost thawing gradients. Environment International 134, 105330.

Zoltai, S., 1993. Cyclic development of permafrost in the peatlands of northwestern Alberta, Canada. Arctic and Alpine Research 25, 240–246.